Environmental Science Nano

Accepted Manuscript

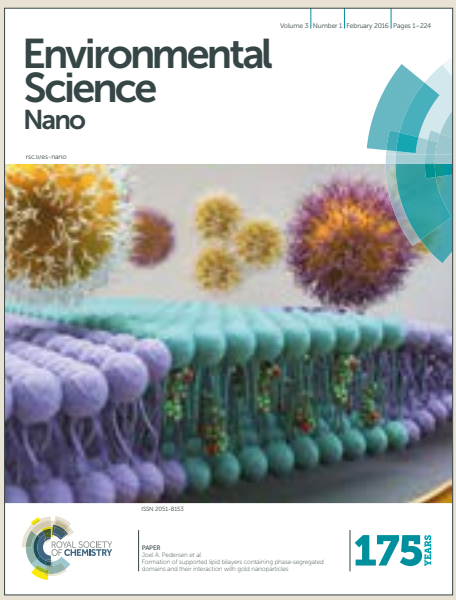

ROYAL SOCIETY OF CHEMISTRY

rsc.li/es-nano

MANUSCRIPT TITLE:
A STUDY ON THE DEPENDENCE OF BACTERIA ADHESION ON THE POLYMER NANOFIBRE DIAMETER

View Article Online
DOI: 10.1039/C8EN01237G

CORRESPONDING AUTHOR:
Fabrizio De Cesare
Department for Innova4on in Biological, Agro-food and Forest Systems (DIBAF)
University of Tuscia
Via S. Camillo De Lellis - 01100 Viterbo (Italy)
email: *decesare@unitus.it*
ORCID ID: *hAps://orcid.org/0000-0001-9810-8746*

CO-AUTHORS:
Elena Di MaNa, Eyal Zussman and Antonella Macagnano

JOURNAL:
RSC - ENVIRONMENTAL SCIENCE: NANO

ASSIGNED ASSOCIATE EDITOR:
Prof. Iseult Lynch

MANUSCRIPT:
Full Paper

ENVIRONMENTAL SIGNIFICANCE STATEMENT

Nanomaterials and nanostructured topographies have been employed prevalently to reduce the bacterial adhesion in various contexts (medicine, food, and industries). Only nanofibres have been rarely applied to support the colonisa4on by bacteria in energy and wastewater treatment applica4ons. The beneficial effect by nanofibres, here presented, in accomplishing a stable adhesion of bacteria, apparently favoured by the bacteria-to-fibre ra4o, the presence of bacterial condi4oning film, the excep4onal specific surface area of nanofibrous scaffolds together with the employment of biodegradable and biocompa4ble materials could permit to create more efficient, eco-friendly and safe materials (like target-specific bios4mulants and biopes4cides for agriculture, microbial fuel cells, bioreactors and filtra4on systems, selec4ve materials for wastewater treatments, specific biochemical catalysis, materials for biomedicine).

A Study on the Dependence of Bacteria Adhesion on the Polymer Nanofibre Diameter

View Article Online
DOI: 10.1039/C8EN01237G

Fabrizio De Cesare[1,2], Elena Di Mattia[3], Eyal Zussman[4] and, Antonella Macagnano[1,2]

[1]Department for Innovation in Biological, Agro-food and Forest Systems (DIBAF), University of Tuscia, 01100 Viterbo, Italy
[2]Institute of Atmospheric Pollution Research, National Research Council (CNR), 00015 Monterotondo (Rome), Italy
[3]Department of Agriculture and Forestry Science (DAFNE), University of Tuscia, 01100 Viterbo, Italy
[4]Faculty of Mechanical Engineering, Technion - Israel Institute of Technology, Haifa, 3200003, Israel

ABSTRACT

Topography nanostructures have been extensively studied to reduce bacterial adhesion in medical, food and industrial contexts. Fibres have also been used in energy, water and wastewater treatments, and medical applications. Nanosized fibres, however, have rarely been analysed in interactions with bacteria, and they have always resulted as inhibiting bacterial adhesion and proliferation. We discussed here the size effect of polymer nanofibres on the attachment of bacteria. As a model system, a 3D self-standing electrospun nanofibrous poly(ε-caprolactone)-based scaffold was fabricated, and *Burkholderia terricola* bacteria cells were used for testing the interactions. The initial reversible adhesion and the subsequent stable irreversible docking of bacteria to nanofibres through various mechanisms, the orientation of bacteria along nanofibres, and the communication between cells were explored. Bacteria initially attached preferentially to nanofibres with ≈100 nm diameter, *i.e.* an order of magnitude smaller than that of bacteria, resulting in a bacteria-to-nanofibre diameter ratio as large as ≈5. It is worth noting that interactions always occurred between bacteria and nanofibres coated with a conditioning film of organic substances of bacterial origin. The conditioning film, the outer membrane vesicles and the bacterial appendages resulted in having a remarkable role in facilitating the following adhesion of *B. terricola* cells to the electrospun poly(ε-caprolactone) nanofibres. They also permitted bacteria to reversibly and then stably attach to the nanofibrous material and connect and communicate each other to form microcolonies embedded in exopolymeric substances, as an early step towards future biofilm formation. No inhibiting effect of the nanosized fibres on the adhesion, proliferation and vitality of the bacterial cells were observed.

KEYWORDS

Electrospinning of nanofibres, bacterial adhesion, *Burkholderia terricola*, nanotopography, biofilm, biointerface.

1 - INTRODUCTION

There is considerable interest in the interaction and adhesion of microorganisms to surfaces and the creation of biofilm. In the last decades, a multitude of observations in some distinct contexts has demonstrated that microbes mostly live attached to surfaces (sessile attitude) rather than suspended in aqueous solutions (planktonic attitude), as previously believed, to intercept nutrients in flowing media or adsorbed onto the surfaces.[1,2] The evolutionary benefit of the biofilm organisation is that microorganisms can survive successfully in adverse conditions.[3,4] Biofilms can be developed on different types of surfaces including natural (e.g., soil particles, wood, or plant/root tissues) and artificial materials (e.g., metals, plastic, clothes, glass, foods, rubber, silicon and other materials for medical implants).[5]

Both beneficial and harmful effects can derive, however, from the formation of biofilms.[6,7] Therefore, several human applications have aimed at preventing and hindering the development of biofilms, but the microbial endurance to biocides and antimicrobials has caused great concern.[4] Various strategies have been developed on purpose, such as the creation of molecules with biocidal and antimicrobial effects on microbes.[8] Another approach was based on the evidence that the initial and pivotal event of environment colonisation by microorganisms and specifically of biofilm formation is the microbial cell adhesion to surfaces (both abiotic and biotic). Hence, some strategies focused on the hydrophobicity and electric potential of both cells and material surfaces, and the topography (roughness) of substrates, which are parameters that can affect microbial adhesion to surfaces.[9,10] A multitude of studies on roughness motifs and geometrical features from micro- to nano-scale (e.g., grooves, pores, pillars, pitches, scratches, nanoparticles, fibres), arranged in regular or random designs have been tested to understand their effect on bacteria adhesion,[11,12] but there is still disagreement on the results.[13,14] Among the various possible surface topography motifs affecting bacterial adhesion, which is the subject of this work, there is very little research, to date, focussing on the interaction and adhesion of microorganisms to micro- and especially to nanofibres, relative to the scientific literature on the relationships between eukaryotes and nanofibrous mats.[15,16]

A common method to produce nanofibres and nanofibrous fabrices is the electrospinning process.[17,18] Typical fibres produced by electrospinning are within the range from micro- to nano-size diameter and can be produced in many different morphologies,[19,20] for a large number of applications (e.g. sensors, energy, medicine, textile).[21–25] One of the most remarkable properties of electrospun nanofibrous matrix is the tremendous increase in the specific surface area that is possible to obtain by tuning the conditions of processing, the type of solvent and polymer concentration, and the use of copolymers.[26,27] This feature can consequently affect the interaction of microorganisms with fibrous scaffolds, as occurs in microbial fuel cells,[22,28] and contaminant removal applications.[29] However, the prevalent investigations on fibre-microbe interactions mostly concerned with the creation of fibrous scaffolds to prevent bacterial attachment by the employment of compounds inhibiting microbial adhesion and activities[30] and on the release of drugs toxic for microbial pathogens.[31] Nevertheless, the specific interactions of bacteria cells with fibres, the orientations of bacteria cells relative to fibres, the dependence of interactions on the fibre diameters and their combined effects, are still open questions. Most of the studies carried out on the interactions between bacteria and fibres have mostly concerned with fibres with diameters larger than or equal to the bacteria size, i.e. from several hundreds of nanometres to some micrometers.[9,12,32–36]

An interesting research question concerns with the interaction between bacteria and polymer fibres with diameters less than those of bacteria, and specifically <100 nm. Various biopolymers like proteins (silk, gelatin, collagen, etc.), polysaccharides and derivatives (chitosan, polyhydroxybutyrate, polylactic acid, polyglycolic acid, cellulose, chitin) and DNA have been usually employed in electrospinning. Among them, poly(ε-caprolactone) (PCL) is an aliphatic polyester that has been employed as electrospun material for many applications.[37,38] In the present study, PCL was selected because it is a cheap, biocompatible and biodegradable polymer with a slow degradation rate,[39] but mostly because it has already been proven to have the capacity of binding bacteria from incubation media.[40] Specifically, PCL was here employed to create a proper nanofibrous scaffold to be used as a substratum suitable for hosting bacteria, as model microorganisms, to investigate the interactions between these microbial cells and PCL nano-sized fibres. The bacteria employed on purpose, as a model species was *Burkholderia terricola*. *Burkholderia* is a genus of Proteobacteria including both human and plant pathogens, and environmentally remarkable species, and it is characterised by hydrophilicity (contact angle in the range 50°-75°) and electrical properties (negative zeta potential) of its cell surface.[41,42] Specifically, *B. terricola* is a species typical of terrestrial ecosystems, where it is prevalently located in the soil volume attached

and surrounding the plant roots (rhizosphere). Here, these bacteria interact with plants to support their growth and prevent diseases, i.e. the typical properties of the plant growth-promoting rhizobacteria (PGPR).[43] The PCL nanofibrous scaffolds were inoculated with *B. terricola* cells and the dynamics and mechanisms involved in the specific adhesion of the selected bacterial species in both early and following stages of colonisation were studied.

2 - MATERIALS & METHODS

2.1 - Nanofibrous scaffold deposition

PCL-based scaffolds were created by depositing electrospun nanofibres on a rotating collector (400 rpm) to develop 3D self-standing nanofibrous structures (Fig. 1a, inset). The pristine solution was 11.7% (w/w) PCL (45 kDa) in $CHCl_3$:C_2H_5OH; 4:1 (v/v) (anhydrous chloroform >90%, anhydrous ethanol >90%) and all chemicals were purchased from Sigma-Aldrich. The home-made electrospinning setup (CNR-IIA, Italy) consisted of a high voltage oscillator (100 V) driving a high voltage (ranging from 1 to 50 kV), a high power AC-DC (alternating current-direct current) converter, and a syringe pump (KDS 200, KD Scientific).

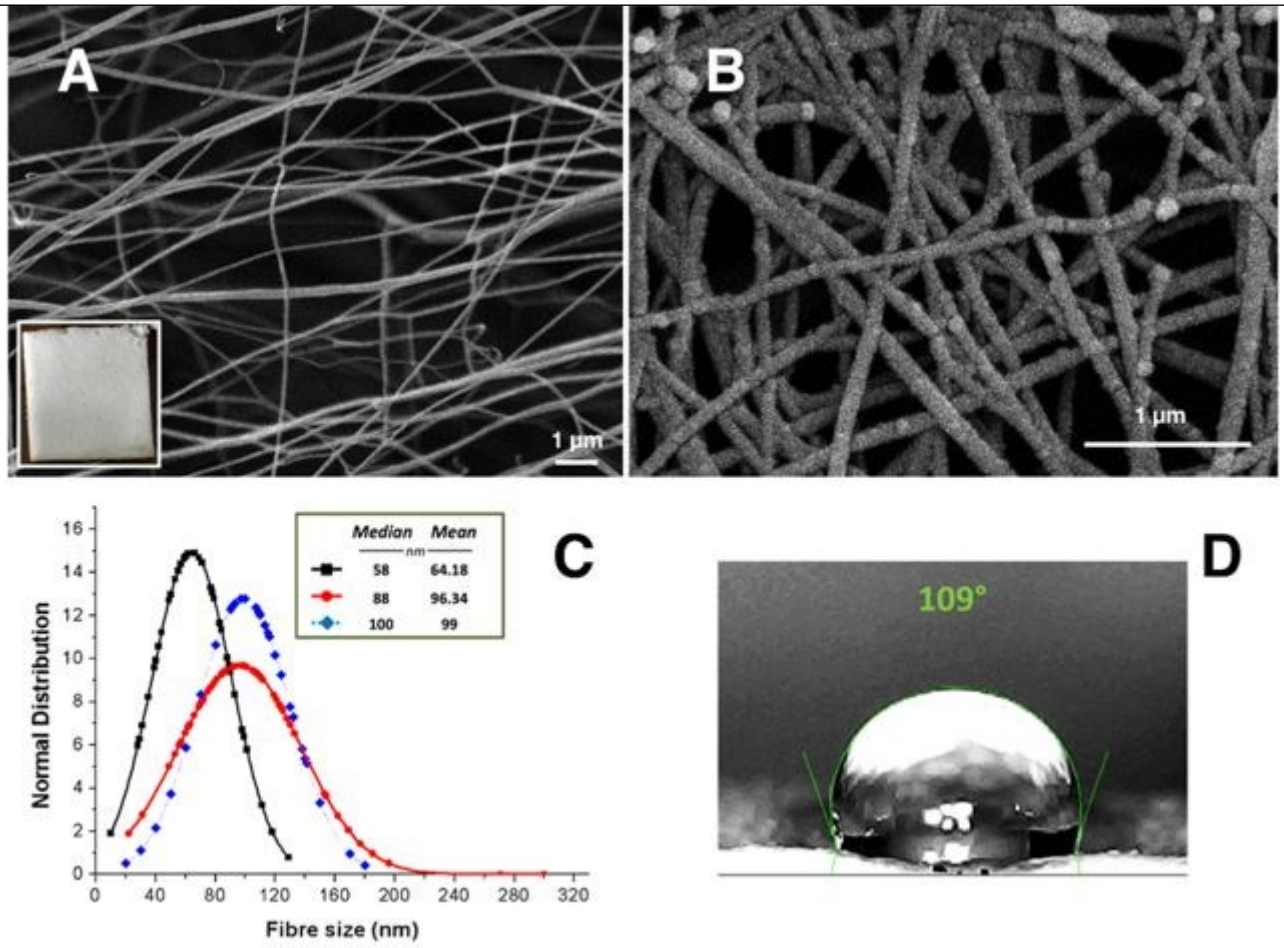

Fig. 1.SEM micrographs of the nanofibrous PCL scaffold: A) soon after electrospun deposition; inset = image of the 3D nanofibrous fabric (1•1 cm) captured by camera; B) after 2 h incubation in the *B. terricola* cells suspension and showing the deposition of the conditioning film onto the nanofibrous framework. C) Distribution of the nanofibres, based on their diameter, measured soon after the electrospun deposition (black line), after CF deposition (red line) and binding *B. terricola* cells (blue line). D) Contact angle of the electrospun nanofabric (drop volume = 8 µl; drop surface = 1.79 mm^2; surface of contact = $6.04x10^{-1}$ mm^2). Scale bars in A and B = 1 µm.

View Article Online
DOI: 10.1039/C8EN01237G

The PCL fibrous matrices were obtained by applying 4.9 kV of electrostatic DC voltage between the tip of a 5 cm long stainless steel equipped syringe and a grounded collector set at distance of 7 cm below the syringe tip and a constant flow rate of the solution 950 µL h^{-1}. A home-made clean-box equipped with temperature and humidity sensors housed the electrospinning deposition. Six centimetre diameter disks wrapped with aluminium foil were used as conductive collectors. The depositions were carried out for 3 h at about 24°C and 30% RH.

2.2 - Contact angle

Water drops (8 µl) were deposited on the fibrous matrix and imaged by a USB-Digital Microscope (2.0 MPx, DIGIMICROSCOPE). Contact angles were measured after 5 s using DropSnake© (LBADSA method), a plugin in ImageJ.

2.3 - Bacteria inoculum and incubation

To analyse the possible interactions between microbial cells and the PCL nanofibres, the electrospun matrices were incubated with cells of the *B. terricola* strain IF25 (presumably assigned to this species) chosen for its PGPR properties and previously isolated from a vineyard soil.[43] The suspension of bacterial cells to be used for producing the active *B. terricola* IF25 cellular population was maintained in liquid culture of Luria Bertani Broth (LB).[44] Before incubation with the electrospun PCL fabrics, *B. terricola* cultures from agar plates were pre-cultured (30 ml) overnight in the LB media and then promptly inoculated in Glucose Mineral Broth (GMB) to obtain a standardised pre-culture to be used in the incubation trials with fibrous matrices. To perform the experimental trial a GMB solution containing (g L^{-1}) 2.2 Na_2HPO_4, 1.4 KH_2PO_4, 0.6 $MgSO_4 \bullet 7H_2O$, 3.0 NH_4SO_4, 2.0 glucose and trace elements was prepared.[45] The incubation of PCL nanofibrous scaffolds and *B. terricola* IF25 cells was performed by inoculating aliquots of bacteria pre-cultured cells in Erlenmeyer flasks containing 25 mL GMB to obtain a suspension of 0.8 ± 0.02 x 106 CFU mL^{-1} (2% v/v final concentration of the inoculum). The interaction of *B. terricola* cells with PCL nanofibres was then assessed by placing 1 cm^2 pieces of electrospun PCL nanofibrous mats into the inoculated flasks and incubating them aerobically and under orbital shaking (80 rpm) in the dark at 30°C for about 30 h. PCL samples housing bacteria cells were collected at 2 h, 4 h and 21 h incubation.

2.4 - Imaging

B. terricola inoculated and non-inoculated samples of electrospun scaffolds collected from suspensions incubated for increasing periods were analysed by SEM and TEM. Briefly, samples were pre-fixed in a solution of glutaraldehyde (2.5% v/v), ruthenium red (0.075% w/v) and lysine acetate (0.075 M) dissolved in cacodylate buffer 0.1 M pH 7.2, before SEM analyses. Fixation in glutaraldehyde (2.5% v/v) dissolved in 0.1 M cacodylate buffer pH 7.2 was then performed for 2 h at 4°C, after cold washings in the same buffer. Post-fixation in osmium tetroxide (2% v/v) in cacodylate buffer for 2 h at 4°C was then performed after washings. Then, a cold rinsing was applied to the processed specimens before dehydration in a graded ethanol series following the critical point method with CO_2 in a Balzers Union CPD 020. Samples were finally sputter-coated with gold in a Balzers MED 010 unit before observations by a JEOL JSM 6010LA electron microscope. Samples for TEM analyses were fixed and dehydrated as for SEM samples and infiltrated with various percentages of LRWhite resin/ethanol mixtures and then embedded in LRWhite resin for 2 d at 50°C. Blocks were cut into ultra-thin sections (60-80 nm) by a Reichert Ultracut ultramicrotome and stained with uranyl acetate and lead citrate. Micrographs were captured by a JEOL 1200 EX II electron microscope equipped with Olympus SIS VELETA CCD and iTEM software.

2.5 - Vitality test (respiration)

The bacteria vitality was assessed by the cell-mediated reduction of a tetrazolium salt following the method of Ladd and Costerton (1990)[46]. Specifically, 2-(4-iodophenyl)-3-(4-nitrophenyl)-5-phenyl-2H-tetrazolium chloride (INT) was used in this study to assess the dehydrogenase activity, which is an expression of the bacterial redox activity (respiration) that bacteria use to obtain the energy for the metabolic and physiological activities[47]. Briefly, to test the bacteria vitality during the incubation of the nanofibrous scaffolds with bacteria, four electrospun PCL samples were collected from batch cultures of microbial populations after 2h, 4 h and 21 h incubation periods. They were then washed in sterile deionised water and placed in flasks containing INT solution (0.01% w/v of redox indicator in 0.1 M phosphate buffer, pH 6.8, and LB 1:20 v/v final dilution) and finally incubated in the dark for 4 h at 30°C, for the colour development. After washing and drying, the PCL pieces with immobilised bacteria were treated with absolute alcohol for the formazan extraction. Absorbance at 495 nm of the resulting solutions after filtration was measured by spectrophotometer (Perkin Elmer Lambda 25 UV-VIS Spectrometer).

3 - RESULTS AND DISCUSSION

3.1 - Nanofibrous scaffolds

SEM images of the pristine 3D self-standing fibrous matrices (≈1 mm thick), showed a relatively smooth surface (Fig. 1a). The distribution of the pristine nanofibre dimensions indicated a mean diameter of 64.18±27nm, a median of 58 nm, and a diameter range of 10-129 nm, while more than 90% of nanofibres were with diameter <100 nm (Fig. 1c). The fibrous matrices were characterised by a remarkable decrease in contact angle with values of 109°±3.8° for pristine PCL nanofibres (Fig. 1d), relative to the typical values (115°-136°) of other electrospun unaligned nanofibrous PCL (pristine). This effect might be due to a higher degree of porosity of the studied system that is usually related to higher hydrophilicity).[48] When incubated with bacteria, however, the fibrous matrices did not maintain the pristine morphology because of the coating with additional organic materials produced by bacteria, as described in §3.2.1, so that the original features of the pristine artificial material were remarkably modified (Fig. 1b). The coated fibres appeared larger in size, in fact, than the pristine nanofibres so that the analysis of the nanofibre population indicated a distribution of their dimensions in the range 22-300 nm, with an average diameter of 96.34±41.21 nm, a median of 88 nm and more than 65% of nanofibres with diameter <100 nm (Fig. 1c). By considering the difference of the average values of the two populations of fibres, pristine and coated, a ≈30 nm thickness on average can be estimated for the fibre coating (see also §3.2.2), then resulting in more than 50% increase in fibre size because of the coating deposition. The coated nanofibres displayed a rough surface with some spheres attached to the nanofibre surface. The contact angle of this coated material as such, however, was not measurable because of the simultaneous presence of bacteria adhering on the nanofibres. The removal of bacteria cells with physical (e.g., stirring, sonication) or chemical (e.g. solvents, biocides) procedures would have altered the features of the coated underneath, then affecting the measures of its contact angle. At the same time, it was not possible to add the coating material without the bacteria, since bacteria produced the coating when in the presence of the PCL fibrous matrix material. These results seem to confirm that the presence of conditioning film (CF) on surfaces can profoundly alter their geometry.

3.2 - Bacteria-nanofibre interactions: Adhesion Phase 1 - Reversible adhesion

In the present study, a number of events related to the adhesion of bacteria cells to the surfaces of the PCL nanofibrous materials were observed from the beginning of the incubation to the end after 21 h. These events were characterised by a series of changes involving both the material and the bacteria and

View Article Online
DOI: 10.1039/C8EN01237G

their mutual interaction described hereinafter. Usually, a successful and stable adhesion of bacteria to both natural and artificial material surfaces results from a series of steps that can drive then the bacteria population to develop a 3D well-organised structure proper of biofilms.[1] The various phases that drive bacteria cells from the planktonic to a stable sessile condition comprehend the approximation and initial contact with an animate or inanimate surface (*reversible adhesion*), firm attachment, interactions between cells and formation of micro- (at first) and macro-colonies (later) (*stable adhesion*).[1] The complex process of adhesion is driven by the activation and expression over time (of incubation, in the present case) of several specific genes that induce modifications in the cells (e.g., flagella removal, pili formation, exopolymeric matrix release and cell envelope modification).[49]

3.2.1 - Conditioning film

SEM micrographs of the nanofibrous scaffolds after 2 h incubation showed an additional organic material deposited onto nanofibres (Fig. 1b). Since no coating material was present on the nanofibres of control samples incubated with the same growth media in the absence of bacteria, and a smooth surface and a smaller average diameter were observed (Fig. 1a), it is reasonable to assign the presence of such conditioning material to *B. terricola* cells. Differently, the nanofibres appeared more homogeneous and larger after 2 h incubation with bacteria, because coated with the organic materials released by bacteria and consequently fused (Fig. 1a,b). In several studies on this topic, the reversible adhesion has been considered only in terms of hydrophobic/hydrophilic interactions between bacteria per se and pristine materials and their relative zeta potential, forgetting that these properties change in the materials as well as in the bacteria depending on several factors, like the growth medium, the environmental conditions, the age, the physiological traits.[3,4] Moreover, the first contact of bacteria with surfaces is rarely occurring (especially in natural ecosystems) with bare surfaces because of the presence of organic compounds in the medium that can heavily affect the pristine properties aforementioned.[50,51] When a surface is exposed to an aqueous natural environment, a film of organic materials (*conditioning film* - CF), in fact, rapidly stick irreversibly (in some seconds to minutes) because of many weak physicochemical interactions.[51] CFs can derive from the incubation media, but they can often be released on purpose by bacteria[50] to modify the surface properties of materials (e.g., hydrophilic to hydrophobic and vice versa, and net electric charge) and then easing their adhesion and the following colonisation.[50,51] As displayed in the SEM micrographs reported in Fig. 2, the CF appeared as a deposit spread over and coating the whole nanoframework. In Figs. 2 and 3 (pink rings and light blue arrows, respectively), the organic deposits also tended to form some kind of membranes when covering several adjacent and intercrossing nanofibres of the electrospun networks. The production of this CF by bacteria could be explained by the opposite features of the two interacting entities in terms of hydrophobicity/hydrophilicity: i) the hydrophobic surface of the electrospun nanofibrous PCL fabrics, and ii) the hydrophilic *Burlholderia* sp. cell surface. It has been reported that bacteria with hydrophobic properties usually prefer hydrophobic material surfaces, while the ones with hydrophilic cell features like hydrophilic surfaces, with a prevalent adhesion of hydrophobic vs hydrophilic bacteria.[41,52] Consequently, the secretion and release of this specific CF by bacteria could be reasonably aimed at modifying the hydrophobic surface of PCL to make it more hydrophilic and then more suitable for interacting with *B. terricola* cell.

Several compounds typically comprise conditioning films in natural (e.g. polysaccharides, lipopolysaccharides, proteins, lipids, nucleic acids, humic substances) and human (albumin, glycoproteins, lipids, lysozyme, phosphoproteins) environments, and these compositions change with bacterial species and within the same strain in diverse environmental conditions (seasons).[50]

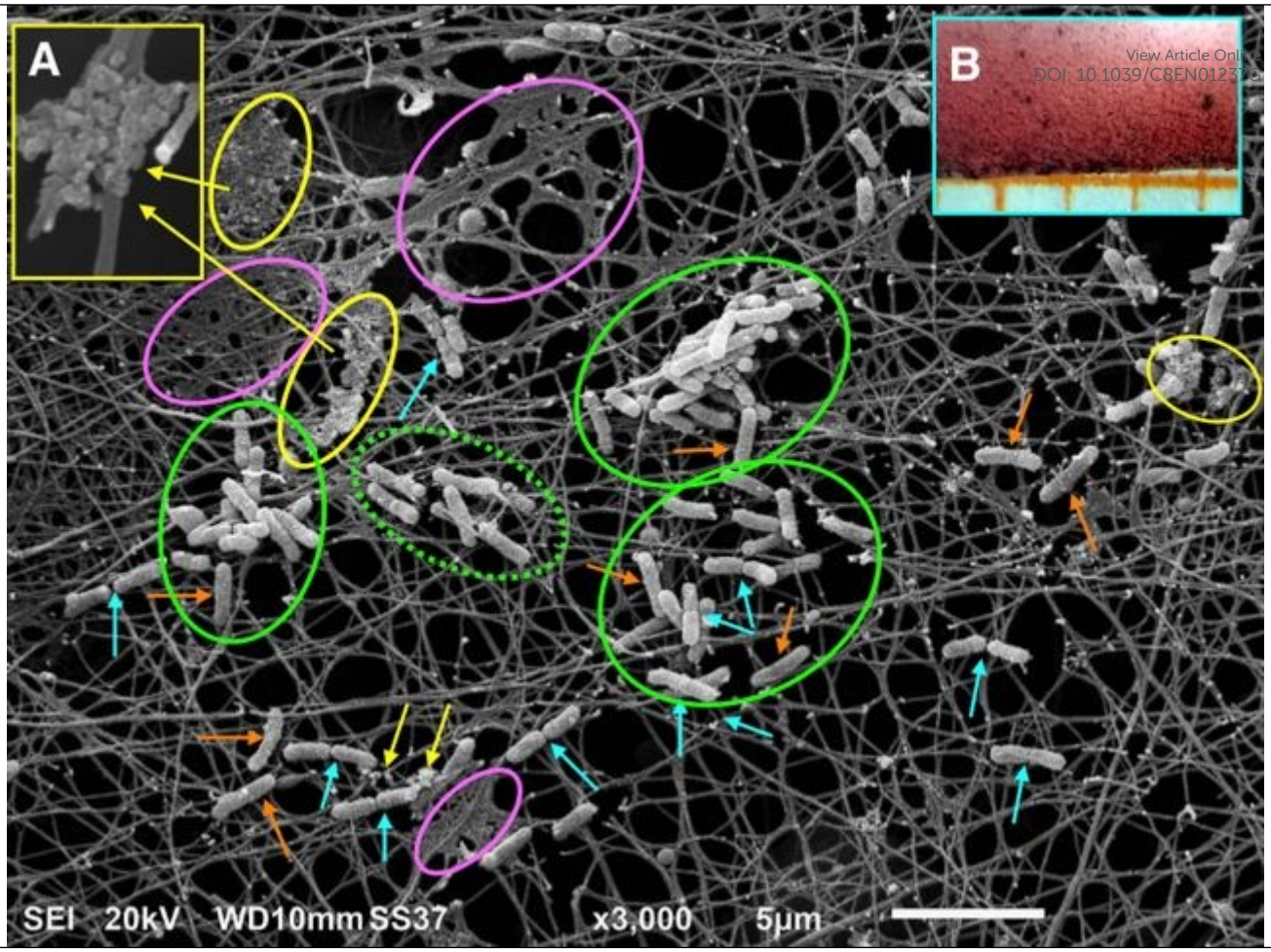

Fig. 2. SEM micrographs of the nanofibrous PCL scaffold after 4 h incubation in the *B. terricola* cells suspension: yellow arrows, circles and inset (A) indicate OMVs deposited onto the nanofibrous network; pink circles = conditioning film forming membranes when deposited onto crossing interlaced nanofibres; light blue arrows = replicating bacteria; orange arrows = elongating bacteria; green circles = cell aggregates and microcolonies (dotted circle identifies a group of cells aligned with single nanofibres except for a cell that moving towards another cell is oriented transversely the fibre) (scale bar = 5 µm). B, electrospun PCL nanofibrous scaffold after 4 h incubation with *B. terricola* cells and testing for bacteria vitality (respiration) (orange grid intervals = 1 cm).

The composition of the CFs is often compared to that of extracellular polymeric substances (EPS) comprising the matrix, but specific studies have demonstrated that it differs when originates from planktonic, capsular, biofilm or lipopolysaccharide (LPS) EPS.[53] In species of the genus *Burkholderia*, polysaccharides are the major components of the CF (named *Cepacian* in *Burkholderia cepacia*),[54,55] although in most bacteria species proteins tend to prevail.[50] Furthermore, the composition of the CF is species specific and can further change depending on environmental and nutritional conditions, and also on the physicochemical properties of the substrate.[50,55] Therefore, the deep knowledge of the specific physicochemical and molecular interactions occurring in the present study between *B. terricola* cells and PCL-nanofibres in a specific moment can only be presumed and needs to be further investigated. Due to the aforementioned difficulties In CF analyses, many studies have analysed the interactions between bacteria and surfaces in the absence of any CF.[56] Notwithstanding, the importance of CFs for bacterial adhesion has been demonstrated in some studies on materials, where surface modification hindering the adsorption of proteins (BSA) also prevented bacterial adhesion.[50] However, other studies reported contradictory results,[54,57] then hampering a consensus on the role of CF as a prerequisite for bacteria adhesion.[58]

View Article Online
DOI: 10.1039/C8EN01237G

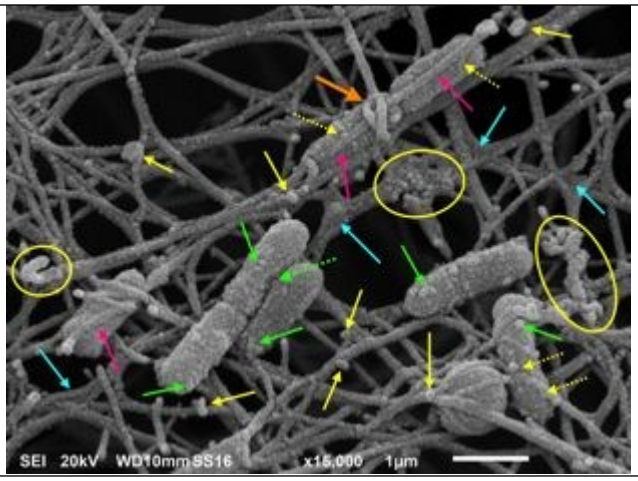

Fig. 3. Type1- and Type2-interactions: SEM micrographs of the nanofibrous PCL scaffold after 4 h incubation in the *B. terricola* cells suspension: yellow arrows and circles = OMVs deposited onto the nanofibrous network (dotted arrows = OMVs involved in the interaction between bacteria and nanofibres); pink arrows = Type1-interactions between bacteria and nanofibres where bacteria cells are aligned along single nanofibres and with the latter running in the middle of the bacteria cells; light blue arrows = conditioning film deposited onto nanofibres, which tends to form membranes onto crossing interlaced nanofibres; green arrows = OMVs generated from the bacteria at cell surface; the orange arrow = a bacteria cell interacting with a single fibre with both Type1- and Type2-interactions: the nanofibre runs longitudinally along the bacteria and two fimbriae protruding from the cell is grasping the nanofibre. Scale bar = 1 µm.

Additionally, the presence of the conditioning material deposition not only dramatically modifies the original chemical and physicochemical characteristics of surfaces such as hydrophobicity/hydrophilicity (wettability), surface charge and free energy, but also the topography of the underlying surface that might be consequently become irrelevant.[51,54] It is worth to note that the CF deposited on the nanofibres and displayed in Figs. 1b, 2 and 3 (see also the following paragraphs and the relative pictures) resulted from the incubation of the electrospun PCL nanofibrous fabrics with bacteria carried out under stirring and from washings for sample preparation for SEM analyses. This fact highlighted that the CF material produced by *B. terricola* cells, though bound unspecifically to the pristine PCL, resulted to be tenaciously bound to the PCL nanofibres underneath. Based on the interactions of bacteria with nanofibres observed in the present study (see §3.2.2), it seems that the CF deposited onto surfaces (and its properties) is confirmed to be the primary driver affecting bacterial adhesion to materials, and in agreement with Garrett et al. (2008).[59] Unfortunately, it was not possible in the series of experiments here carried out to test the adhesion of bacteria in the absence of CF. This organic material, in fact, was released by bacteria themselves when exposed to the nanofibrous PCL fabric and was rapidly adsorbed onto the mat surface as soon as the incubation started, and its chemical or physical extraction would have required previous bacteria removal and preservation of the PCL scaffold, i.e., conditions that would be difficult to perform without mutual alterations. However, some preliminary results obtained in another set of experiments exploiting distinct experimental strategies using the same bacteria strain and electrospun PCL nanofibrous mats seemed to support this hypothesis, because the same but uncoated material appeared to be unable to support bacteria adhesion (data not shown). Consequently, it might be concluded that the presence of CF is a prerequisite for *B. terricola* adhesion.

3.2.2 - TYPE1-Interaction

In the present study, diverse types of interactions between *B. terricola* cells and nanofibres were observed in both SEM and TEM micrographs captured from electrospun nanofibrous scaffolds after incubation in the bacteria inoculated medium (Figs. 2, 3 and 4). It is known that the adhesion of

bacterial cells to surfaces generally takes place following the CF deposition, and it occurs through distinct steps involving unspecific and specific mechanisms, both originating essentially from weak bonding like physicochemical (electrostatic, Van der Waals, and acid-base interactions) and hydrophobic interactions.[1,49] These ties occur, in both natural and most of the artificial environments, between bacteria and the surfaces coated with the various compounds of the CFs (e.g., proteins and polysaccharides).[50,53,60,61]

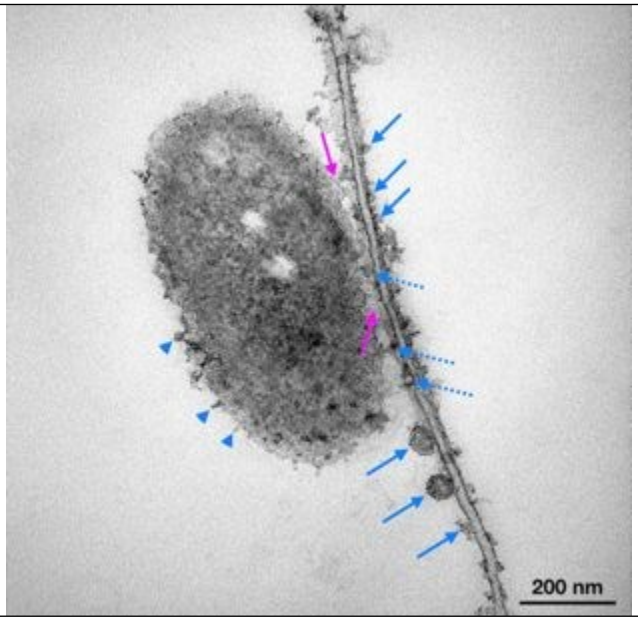

Fig. 4. Type1-interaction: TEM micrograph of a single bacteria interacting with a single ≈30 nm diameter nanofibre: pink arrows = gel like amorphous materials involved in the reversible adhesion of the cell onto the nanofibre; blue arrows = OMVs sited on the nanofibre and in the space between the bacteria and the nanofibre (dotted); blue arrowheads = OMVs generated from the bacteria cell surface. Scale bar = 200 nm.

Since these types of bonding are weak, they are unstable and short-range effective and then reversible, especially under agitation or in flowing media, as it is the case for the experiment carried out in this study. These interactions, then, do not permit a stable relationship between bacteria cells and surfaces and their colonisation, and host infection, in the case of biotic surfaces, until they do not become more stable. Adhesins mediate both types of mechanisms, then the main difference between the two types of mechanisms mostly is the distance they operate.

Figs. 2, 3 and 4 displayed SEM and TEM micrographs captured after different periods of incubation. Fig. 2 but mostly Figs. 3 and 4 (pink arrows) clearly showed a close contact between bacteria cells and nanofibres, typically a surface-to-surface interaction, which was here identified as Type1-Interactions. In these micrographs, this type of interaction seemed to be mediated by a sort of gel-like amorphous materials surrounding *B. terricola* cells (maybe classifiable as capsule-like material) (Figs. 3 and 4, pink arrows). Noteworthy, in the TEM micrograph, the cross-section of the bacteria-colonised nanofibrous scaffold consequent to the preparation of TEM samples resulted in a longitudinal cut not only of a bacteria cell but also of a 30 nm diameter nanofibre (Fig. 4). This TEM micrograph not only provided the visual evidence that very thin nanofibres were generated during the electrospinning deposition and that they were coated by a ≈30 nm thick conditioning film but more interestingly allowed the analysis of the interactions between *B. terricola* cells and proper thin nanofibres (next paragraphs). Specifically, the capsule-like material of *B. terricola* cells seemed to merge with the CF and deposited onto the nanofibres. Furthermore, in some cases, the bacteria cells looked like not only laying on the conditioned nanofibres but almost surrounding them with their capsule materials all along the area of contact (Fig. 3,

pink arrows). By the way, some species of the *Burkholderia* genus have been reported to release materials as CFs during the initial phases of biofilm formation that are composed of polysaccharides and proteins[53] and then have been supposed to be chemically similar to those of capsules.[62,63] Therefore, the adhesion of *B. terricola* cells to nanofibres here observed seemed resulting from the interactions between macromolecules present in the capsule-like material and the macromolecules comprising the bacterial CF.

To understand the type of mechanisms involved in the interactions hereinabove described, unspecific mechanisms generally include van der Waals and repulsive electrostatic forces and work over distances of several tens of nanometers (>50 nm).[64] This type of mechanisms mostly involve macromolecules, which act as adhesins, sited both outer than and within the bacteria cell wall such as polysaccharides, lipopolysaccharides and non-fimbrial proteins),[61] and typically occur with inanimate surfaces.[61,65] Differently from the unspecific mechanisms, the short-range stereochemical interactions of the specific mechanisms (ligand-binding) typically occur with biotic but also with abiotic surfaces and involve adhesins (lectins) participating the molecular recognition between ligand and receptor molecules (distances <5 nm, with the involvement of hydrogen bonding, ionic and dipole-dipole interactions, and hydrophobic interactions).[61] These specific interactions with abiotic surfaces of artificial materials mostly occur when these surfaces are coated with CFs, especially if including adsorbed proteins.[60] These adhesins can be both non-proteinaceous and proteinaceous. Non-proteinaceous adhesins can be present on the bacterial cell surface (non-pilus or non-fimbrial adhesins) and include polysaccharides and microbial surface components recognising adhesive matrix molecules (MSCRAMM) clumping factors.[66] Conversely, proteinaceous adhesins comprise a large group of high molecular weight proteins located on the bacterial surface.[66,67] By the way, the presence of non-proteinaceous and proteinaceous adhesins like LPS and lipoproteins has also been described in *Burkholderia* spp. and, as said, can be present in the capsule material.[63] Based on what is displayed in Fig. 4, interactions between the microbes and the artificial material seemed to occur at much less than 50 nm distance, if the surfaces of *B. terricola* cells and nanofibres were considered, but actually occurred in the space around these two surfaces where the capsule-like and CF materials merged, i.e. with no solution of continuity. Hence, they could be explained by the presence of short-range stereochemical interactions typical of the specific ligand-binding mechanisms of adhesion. The knowledge of the exact nature of the interactions occurring between *B. terricola* cells and nanofibres will require the analysis of the composition of both the CF and the capsule-like material that is difficult to carry out in the experimental conditions here used. It is worth to note that regardless of the unspecific or specific interactions between bacteria and conditioned nanofibres (Figs. 2, 3, and 4) they were observed after an incubation period performed under stirring and after washings for sample preparation for SEM and TEM analyses. Then, despite their weakness, the bondings resulted in being strong enough to maintain bacteria attached to nanofibres during agitation. Since the specific mechanisms are usually typical of a more stable type of interaction between bacteria cells and substrates, a transition from reversible towards irreversible adhesion is already occurring.

3.2.3 - Outer membrane vesicles (OMVs)

Interestingly, the analyses of both SEM and TEM micrographs of the colonised electrospun nanofibrous PCL fabrics after 4 h (Figs. 2 and 3) and 21 h (Fig. 4) incubation pointed out also other details concerning the dynamics of processes occurring during the reversible phases of the Adhesion Phase 1. As shown in Fig. 4, the colonised nanofibrous scaffolds upon cutting for TEM imaging highlighted the presence of some circular structures (disks) in the micrograph reported therein. These disks represented cross sections of outer membrane vesicles (OMVs), i.e. nanoscale spherical structures of bacterial origin. The OMVs are usually produced by several species of Gram-negative bacteria and are generated from bulges

protruding from the outer membrane (OM) of cells. The following fission of these excrescences produces spherical vesicles that are then released in the outer space.[68] OMVs were shown in both TEM and SEM micrographs (Figs. 2, 3 and 4), where they appeared as closely associated to *B. terricola* cell surface, and specifically as lumps generated by bacteria and distributed on the whole cell surface in various size (Fig. 3 green arrows; Fig. 4 blue arrowhead). In SEM micrographs, OMVs were visible in vast amounts (Figs. 2 and 3) and appeared as granular deposits, piles and aggregates (Figs. 2 and 3, yellow rings and arrows and inset in Fig. 2) distributed throughout the surface of the nanofibrous PCL framework. OMVs have been observed to be generated by bacteria in both planktonic and biofilm mode, on both solid and liquid media, as well as in swarming cultures, and are produced in all growth stages and various natural environmental conditions, and they have finally been related to both inflammatory events and stress conditions.[69]

In Fig. 4, OMVs appeared as electron-dense disks. Because of the generation from the outer cell membrane, OMVs present an external double-layered membrane (here visible in the larger vesicles as two parallel dark and white circles - Fig. 4) and contain periplasmic compounds in their lumen (virulence factors, communication signals, and nucleic acids), so that they appeared as electron-dense material by TEM.[68] As shown in SEM and TEM micrographs, OMVs released by *B. terricola* cells displayed a broad size range, from tiny (≈20 nm) to large (≈300 nm) diameters (Figs. 3 and 4, yellow and blue dotted arrows). Several publications have demonstrated, in fact, that the population of OMVs released by bacteria in distinct contexts show a broad distribution of diameters from 10 to 300 nm.[69]

Many roles have been assigned to OMVs in microbial ecosystems in different contexts. OMVs have been proven to be standard constituents of biofilms, contributing by about 20-30% of the whole matrix proteome (in *Pseudomonas aeruginosa*), and participate their formation.[70,71] OMVs can also be significantly different in both the quantity and quality in distinct physiological states (planktonic vs sessile forms).[70] This result would explain the different size of OMVs observed in the various SEM and TEM micrographs (Figs. 2, 3 and 4, yellow, green and blue plain and dotted arrows) as well as the variable electron-density between the small and larger OMVs.[71] Moreover, OMVs can mediate the delivery of growth factors and components (e.g. proteins and DNA) participating the extracellular matrix organisation of biofilms.[72]

OM vesicles also seem to take part in the communications between bacteria cells (quorum sensing) that are necessary for the development of mature biofilms.[68] These features might explain the role of OMVs also in the present study, where an artificial ecosystem for bacterial adhesion and colonisation was recreated. In detail, two possible roles for OMVs could be presumed for example based on their localisation in the colonised nanoframework: i) adhesion and ii) aggregation. In SEM micrographs, OMVs appeared attached to the nanofibres (Figs. 2 and 3, yellow rings and solid arrows, as well as the inset in Fig. 2). Furthermore, *B. terricola* OMVs, whatever their size, appeared in TEM micrographs as adhering directly to the nanofibre surface comprising the electrospun PCL mat, i.e. without the mediation of the CF (Fig. 4, solid blue arrows), suggesting that OMVs independently from diameters shared a similar composition of the external surface. Noteworthy, these pieces of evidence also suggested that the OMV release is an event preceding CF deposition and that the OMV content might be responsible for CF formation on surfaces. Interestingly, OMVs also appeared, in both SEM and TEM micrographs, to be present in close contact with both *B. terricola* cells and the electrospun PCL nanofibres (Fig. 3 dotted yellow arrows). Specifically, the TEM analysis of the colonised nanoframework displayed for the first time, to our knowledge, that OMVs were localised in the interface between the bacteria cells and the nanofibres (Fig. 4, dotted blue arrows), thus demonstrating the possible role of OMVs also in the adhesion of bacteria to abiotic materials (electrospun PCL nanofibres, in this case). Here then, OMVs could facilitate the interactions between the cells and the artificial surfaces by directly acting as bridges or by releasing their contents (maybe proteins) that could serve as both linking and cementing agents

(adhesins). Some studies associated the role of OMVs to bacterial adhesion to surfaces, but all of them concerned the specific interactions of the microbes with animated cells and ascribed to OMVs a role in the infection processes.[69,70] Furthermore, in OMVs of *P. aeruginosa*, it has also been demonstrated that hydrophobic molecules such as 2-heptyl-3-hydroxy-4(1H)-quinolone (PQS) are present at cell surface,[73] and might then facilitate the interaction of bacteria cells with hydrophobic surfaces like that of the present electrospun PCL mats. *Burkholderia* species are known to produce molecules similar to PQS (AHQS), in fact, but their association with OMVs is still to be demonstrated.[74] In any case, no publication has reported, to date, any information about the role of OMVs in the adhesion of bacteria to inanimate artificial surfaces and mostly to nanofibres, to our knowledge.

These findings, in our opinion, might have great potential effects in applications where facilitation, retardment or hindrance of bacteria adhesion are required. Such information, for example, might offer the opportunity to develop new classes of effectors (from antimicrobials to growth promoters) that could inhibit the adhesion of pathogens to implants and reduce the infectious diseases by acting on the release of OMVs by bacteria, modifying the OMVs surface properties and tuning the cargo capacities of OMVs. Oppositely, these effectors could stimulate the attachment of beneficial bacteria on supports created on purpose for environmental and agricultural applications by using the same strategies. As concerns the role of OMVs in bacteria aggregation, OMVs were observed in SEM micrographs at the interface between adjacent bacteria, presumably acting as bridges joining the cells (Fig. 3, dotted green arrow). In *Helicobacter pylori*, it has been observed that proteins present at OMV surface are involved in linking bacteria cells to form biofilms.[75] However, a similar observation in *Burkholderia* species has not been reported, yet, to our knowledge. Then, a possible role for *B. terricola* OMVs in both the initial stages of the bacteria cell adhesion to the nanofibres of the electrospun PCL, as an artificial material, and the cell aggregation for the development of biofilm might be suggested, and could be then of utmost importance in the development of materials suitable for either preventing or favouring biofilm formation.

3.2.4 - Cell-to-fibre adhesion and orientation (alignment)

After 4 h incubation, regardless of mediation of the diffused CF coating the entire nanofibrous framework and the multitude of OMVs spread throughout it, single cells of *B. terricola* appeared as adhering to nanofibres and started replicating and spreading onto the nanofibrous framework. Consequently, bacteria cell clusters adhering and growing on the electrospun PCL nanofibrous scaffolds began forming (Fig. 2). As visible in this SEM micrograph, bacteria cells at this stage of colonisation of the nanofibrous fabric showed a high degree of activity, as it is suggested by the diffused presence of longer, replicating and just duplicated bacteria cells (Fig. 2, light blue arrows = early duplicated cells; orange arrows = long cells, before division). Such evidence was further confirmed by testing the metabolic activity (redox activity - respiration) activity[47] of the nanofibrous scaffolds after bacteria colonisation. Inset B of Fig. 2 shows that high metabolic activity was already present after 4 h incubation especially in the most external portions of the scaffolds which were more exposed to the incubation media and intercepted at first the planktonic cells and were then early colonised. The respiration assay here used is generally related to the global metabolic activity (cell energy production), and it commonly points out only cells that are metabolically active, then it was preferred to the live/dead assay, which is usually employed in these types of studies. The latter assay, in fact, could include cells that are alive but not metabolically active (e.g. spores and damaged cells), so that although they resulted positive to the assay, they would not effectively participate to any activity of interest in target applications for which they had been employed.

It is interesting to note that, as it is visible in Fig. 2 and more clearly observable in Figs. 3 and 4, *B. terricola* cells preferentially attached, as initial contact, to single PCL nanofibres aligning along them, i.e.,

laying on them and orienting their longitudinal axis in the same direction of the nanofibres. Intriguingly, the bacteria appeared mostly laying on these nanofibres, so that the cells looked as longitudinally crossed by the nanofibres. Amazingly, Fig. 3 displayed the frequent perfect centring of the fibres relative to the bacteria cells and their alignment, like train wagons on a railway (pink arrows). This finding seems to contrast with what reported in the little number of original research studies published to date (only 6 to our knowledge) somehow investigating the possible interactions of microorganisms with fibres and their types of adhesion based on this topography motif (Table 1).[12,29,32–35]

To evaluate this issue and identify a parameter (or index) that might be related to these discrepancies, the dimensional relationship between the diameters of the electrospun nanofibres and the various species of bacterial cells were expressed as bacteria-to-fibre diameter ratio (BFR).[64] In the present study, the CF coated nanofibres ranged from 22 to 300 nm (average value 96.34 nm) and then the expected BFR values were in the range 22.7-1.7 (average value 5.2 nm), since they were much smaller than *B. terricola* cells (≈1.5 µm length; ≈0.5 µm width) (Fig. 1c). Interestingly, the bacteria appeared instead not to adhere to nanofibres of any size, but they always explicitly interacted with those of 20-180 nm diameter, and prevalently with those of 99 nm width (Fig. 1c). Taking into account the distribution of fibres where the preferential adhesion of bacteria was recorded (Fig. 1c), the consequent distribution of BFR values was $2.8 \leq BFR \leq 25$, with an average real BFR values as large as 5.1, i.e. much higher than those reported in the above mentioned studies on the interactions between bacteria and fibres (with one exception), where BFR values were in the range 0.08-7.1, because of the much larger size of the fibres tested (Fig. 1c; Table 1).[12,29,32–35] These results could be of extreme importance in fixing the standards for electrospun nanofibrous PCL materials suitable to induce adhesion or repulsion against bacteria, according to target applications.

The 3D structure of the non-woven nanofibrous PCL framework prevalently exposed the outer portion of this porous nanostructure to the contact with bacteria during the incubation so that *B. terricola* cells appeared to interact with external nanofibres and bacteria cells mostly appeared as suspended on single tiny nanofibres or groups of them (Figs. 2, 3 and 4) (see also §3.2.5). However, because of the stirring incubation, the role of the electrospun mat was not to act as a nanonet passively collecting bacteria from the incubation media, as in filtration applications, but to behave as an active nanoweb attracting bacteria cells inducing their adhesion.[40] As concerns the orientation of *B. terricola* cells relative to fibres at this early stage of interaction and when direct interactions occurred (i.e. not mediated by the relationships with other cells like in microcolonies), they mostly appeared, as said, aligned along the longitudinal axis of the electrospun PCL nanofibres, notwithstanding the little dimension of the latter relative to the bacteria diameter (Figs. 2, 3 and 4) and they also crossed other fibres as a consequence of the main fibre crossing the network, and consequently colonised the interspaces (Figs. 2 and 3) (see also §3.2.5). TEM micrograph reported in Fig. 4 confirmed as well the alignment of bacteria cells along the electrospun PCL nanofibres and also displayed the interaction with a tiny nanofibre (≈20 nm) so that the BFR resulted even as large as 25. These findings, then, seemed to contrast with the suggestions of Kargar et al. (2012) who concluded that bacteria adhering on and aligning with the fibres was the most unfavourable condition for bacteria adhesion to fibrous substrates based on a mere energetic explanation.[12] They explained that the lowest alignment with fibres vs the prevalent alignment with the spacing between fibres was due to the reduced number of binding sites for adhesion in the former case. Curiously, however, the same authors reported that when the fibre diameter was less than the bacteria diameter, bacteria cells aligned prevalently onto the fibres, although they ascribed this result to the interaction of bacteria with the substrate underneath the nanofibres. The present study, then, agrees with the paper of Kargar et al. (2012) as concerns the primary orientation of bacteria along thin fibres but contrasts with the preferential interaction with 100 nm nanofibres here clearly demonstrated regardless of the mechanisms responsible for that.[12] It seems evident that the energetic explanation of

Kargar and co-workers in the adhesion dynamics between bacteria and fibres is not the only principle that drives the interactions between the two entities. Moreover, although laying on nanofibres much smaller than the cell diameter (3.3<BFR <25), *B. terricola* cells never showed any kind of distortion in the present study (Figs. 2 and 3), as it was reported instead in the article of Abrigo et al. (2015) with BFR values in the ranges 7.1-0.45 and 1.7-0.17, respectively, without considering the presence of CF.[32] It is worth to note that also in the very recent studies of Tamayo-Ramos et al. (2018) and Rumbo et al. (2018), the PCL fibres used (similarly to the present study) to test the colonisation by some bacterial species displayed a much larger diameter (Table 1) (then properly classifiable as microfibres) than in the present study, and much lower BFR values, relative to the microbes tested.[35] Then, in all of the published studies aforementioned, the beneficial effect of fibres claimed as favouring bacterial colonisation could not be compared with the promising results here presented, where proper nanoscale fibres were tested. At the same time, the inhibiting effect on the bacterial colonisation induced by the curvature of fibres with little diameter as claimed by Abrigo et al. (2015) and Kargar et al. (2012) seemed not here to be observed at all.[12,32]

Because of the contrasting results between this study and those aforementioned, the effect of other topography motifs and roughnesses of surfaces like scratches, ribbons, crevices, pits, tubules, ridges, lines, and grooves on the adhesion of bacteria reported in the published literature were analysed. Most of these studies highlighted that the higher the surface for interaction with single bacteria and the higher the adhesion to surfaces, and vice-versa.[76] Only a few studies analysed the effects of roughness motifs of nanometre size on bacteria and reported that these cells tended to align prevalently with the grooves if the spacing in the motifs was comparable with the diameter of bacteria.[76] When the roughness motifs were much smaller than the bacteria diameter, a general inhibition of adhesion and colonisation was observed, with no bacteria aligned along the various topography units, but crossing or laying aside the scratches or other motifs.[77] In any case, in all of the publications on the effects of linear nanotopography on bacteria adhesion, bacteria cells (especially the rod-shaped) were never reported to stay along (on top) of these structures, to the best of our knowledge. In some studies employing pillars, posts, hair-like structures and wires of nanometre size as surface topography motifs interacting with bacteria, contradictory results were reported. These structures often reduced the adhesion of bacteria to surfaces,[77] so that a very efficient bactericidal activity was observed in a study with black silicon (a synthetic analog of insect wings and gecko skin structures), characterised by specific nanopillar size (<300 nm height), tip diameter (≈ 60 nm) and spacing between the motif units (≈ 60 nm).[78–80] On the contrary, when surfaces decorations with pillars or similar nanoarrays presented a spacing large enough to host bacteria, these microbial cells preferred the vertical attachment to the nanopillars than staying in the pitches.[81–84] In these cases, the interaction and orientation of bacteria cells onto similar nanopillars resembled that one observed in the present study between bacteria and nanofibres and the relative dimensional ratios between bacteria and these fibre-like topography units (named bacteria-to-fibre-like diameter ratio - BFR_{like}) were in the range 0.6-2.3 (Table 1). Surprisingly, comparing the observations of Jeong et al. (2013) with those of the present study, *S. oneidensis* seemed to interact with and orient on nanopillars (used in that article) similarly to the way of *B. terricola* with nanofibres here reported, despite the different values for BFR and BFR_{like}[83]. In a fantastic picture reported in the same article, S*. oneidensis* cells grasped at a nanopillar with their pili very similarly to the way a *B. terricola* cell displayed in Fig. 3 (orange arrow) did with an electrospun PCL nanofibre using its fimbriae. In the aforementioned articles bacteria also tended to stay on the vertical structures than on the pitches. Preliminary studies showed that *B. terricola* cells at the early stages of incubation and in experimental conditions similar to those here described seemed to perceive the topography of the underlying nanoframework so that they preferred to adhere to thin nanofibres than larger ones and to other more flat surfaces (data not shown). The adhesion of bacteria cells to nanopillars and their

alignment along them reported in the papers of Hochbaum et al. (2010), Jeong et al. (2013), Sakimoto et al. (2014) and Leonard et al. (2017) clearly resembled those of *B. terricola* to nanofibres as linear nanotopography motifs described in the present study, although the relative BFR_{like} values were much lower than the BFR values here calculated (Table 1).[81–84]

It is worth to note that in the present study the colonisation of nanofibres was comparable or greater than those reported in the cited papers (although the difficult comparison due to the different times of incubation and unknown inoculum and incubation conditions applied therein) (Fig. 5). Based on the fact that a population of nanostructures with varying dimensions were here present in the same experiment, opposite to most of other studies on both nanofibres and pillars-like structures, the calculated BFR (or the BFR_{like}) index here suggested might be a promising parameter to compare the capacity of linear structures (nanofibres, posts, pillars) of interacting with bacteria cells in the same experimental conditions. It is worth noting that comparable conditions should include the presence or absence of CFs on the nanotopography motifs. Consequently, the discrepancies with other studies testing bacteria-fibres interactions previously mentioned might depend on the very large nanostructures tested therein (BFR <1) and on the absence of CFs on them so that the analysed interactions of bacteria with artificial materials were limited to the mere physical and physicochemical relationships between the only two entities rarely occurring in real ecosystems, both natural and anthropic. It is our opinion that the preferential adhesion on nanofibres here observed resulted from the combination of topography (nanofibres) and chemical features of the material (PCL hydrophobicity modified upon electrospinning and CF deposition by *B. terricola* cells) and bacteria cells (*B. terricola* surfaces and OMVs) and environmental conditions (growth medium, temperature and stirring), with CF deposition being the most critical parameter. Differences, however, might also be observed in bacteria species with different shapes, e.g. spherical (e.g. *Staphylococcus* genus) instead of rod-like.

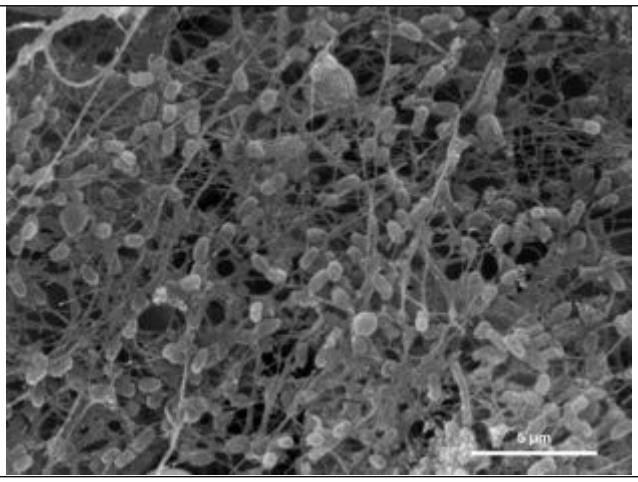

Fig. 5. SEM micrograph displaying the extensive growth of *B. terricola* cells onto the electrospun PCL nanofibrous scaffold after 21 h incubation. Scale bar = 5 µm.

3.2.5 - Cell-to-fibre interactions in cell motility

At early stages of colonisation of the nanofabrics, e.g. within 4 h incubation, it seemed that as soon as *B. terricola* cells adhered to nanofibres, they started replicating on the fibres and spreading throughout the electrospun nanoframeworks. The alignment of cells along trains on nanofibres and their orientation with some visible distortion towards specific zones of aggregation with the formation of cell clusters suggested the presence of diffused motility of cells (Fig. 2). SEM micrographs suggested some possible movements of bacteria on the nanofibres probably consequent to social behaviour inputs. Bacteria cells, in fact, looked as "sensing" the presence of other cells, appeared as distorting their body, orienting

View Article Online
DOI: 10.1039/C8EN00237G

towards other cells and moving in their direction to aggregate in microcolonies (Fig. 2, green circles). Bacteria cell communication, in fact, is mostly driven by quorum sensing, an intercellular signalling system coordinating and regulating the behaviour of bacteria adhering to surfaces that is based on the perception of the population density by the production and extracellular release of specific compounds.[85] These molecules accumulating in the surrounding environment trigger, above a threshold concentration, the activation of genes.[51] Quorum sensing has been claimed to be involved, for example, in the regulation of motility, the production and release of EPS and other exoproducts and the process of detaching.[51] The proximity to other individuals seemed here to be perceived by *B. terricola* cells laying onto and aligning along nanofibres that abandoned this configuration and changed directions towards other bacteria nearby. They appeared then orienting transversally to the nanofibres and crossing other nanofibres to reach other cells (Figs. 2, 3 and 6). In Fig. 2 (dotted and solid green rings), this event is evident in the cells that have bending bodies or look like oriented differently from the others (that are aligned along the nanofibres) and mostly obliquely to nanofibres. The final result of this moving is that *B. terricola* cells often looked like tightrope walkers marching on suspended nanofibres and colonising the rest of the nanofabrics.

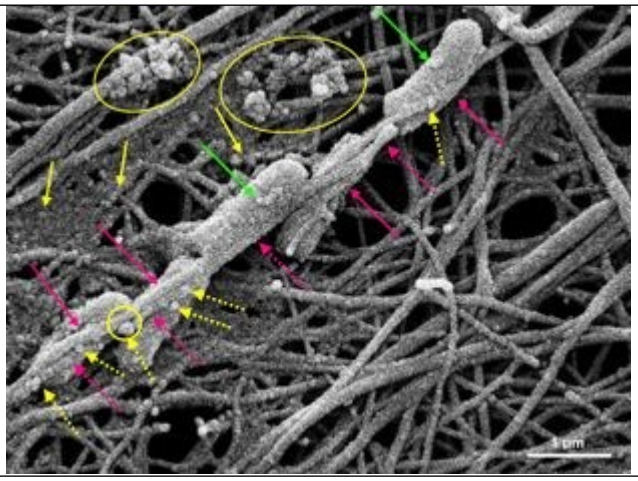

Fig. 6. SEM micrograph of the nanofibrous PCL scaffold after 4 h incubation in the *B. terricola* cells suspension: yellow arrows, circles indicate OMVs deposited onto the nanofibrous network (dotted arrows indicate OMVs embedded in the slime and associated with OM tubes generated by bacteria); purple arrows = nanofibre wrapping bacteria cells (dotted arrows indicate possible slime trials and OM tubes generated by bacteria); blue arrows = OMVs adhering to nanofibres, in the interspace between bacteria and nanofibres, and on the cell surface of bacteria soon after their generation; green arrows = OMVs generated on the bacteria cell surface. Scale bar = 1 µm.

However, the apparent quite total absence of any visible appendage in the micrographs captured at this stage of incubation (except for what documented in Fig. 3, orange arrow) suggests that this apparent motility was driven by mechanisms other than those depending on the presence of appendages. Among the known mechanisms supporting bacteria motility on surfaces those that are independent of the presence of any appendage are *gliding* and *sliding*, typical of some bacteria species. Gliding is described as the movement along the longitudinal axis of rod-shaped bacteria (typically myxobacteria) carried out through inner membrane motors localised along a helical track within the cells and causing a clockwise rotational movement that brings bacteria forward. This moving system also uses a trail of extracellular matrix (ECM) (a polyelectrolyte gel also called slime) to maintain the contact with the substrate.[86] In sliding, instead, bacteria (typically mycobacteria) generate colonies spreading passively away from the colony centre as a result of the expansive forces due to cell growth, prevalently along the longitudinal axis of cells, facilitated by the presence of amphiphilic molecules located in the outermost layer of the cell envelope, such as glycopeptidolipids.[87] However, both gliding and sliding have never

been observed in the genus *Burkholderia*, although some species are known to produce biosurfactants (such as rhamnolipids) and some slime that are known to be involved in sliding and gliding, respectively.[88] Intriguingly, the disposition of some bacteria cells as twisting along and with nanofibres, instead of the perfect alignment and centring of the nanofibre relative to the bacteria previously described in Fig. 3 (orange arrows), seemed to suggest a rotational movement of an object attached to an unfixed rope (Fig. 6, solid pink arrows), then suggesting bacteria moving according to the gliding motility features. Noticeably, several OMVs were also present associated with a material surrounding the nanofibre similar to the slime trail (maybe corresponding to or derived from the CF) or the OM tube typical of gliding (dotted yellow arrows) (Fig. 6). By the way, the presence of OM tubes and OMVs embedded in slime trails have been described in gliding motility, as structures containing signals promoting the specific recognition of adhesion sites and facilitating the trail following.[89] Therefore, the possible motility of *B. terricola* cells at this time of incubation, apparently not mediated by appendages, might be explained, in principle, by the mechanisms described for gliding motility. In this case, it would be the very first time for gliding to be anyhow associated with the motility behaviour of the *Burkholderia* genus. More research is consequently required to confirm this observation.
In conclusion, it seems that also the social behaviour and motility of *B. terricola* cells here observed seemed to be influenced by the presence of the nanofibrous substrate. Such social actions involving bacteria and nanofibres have never been reported to date, to our knowledge.

3.3 - Bacteria-nanofibre interactions: Adhesion Phase 2 - Irreversible adhesion

3.3.1 - TYPE2 Interaction (fimbriae-mediated)

After 21 h incubation, a more stable attachment of bacterial cells to electrospun nanofibres was observed in bacteria-colonised PCL nanofibrous fabrics that seemed to be due to appendages (Fig. 7, orange arrows). Adhesion, in fact, is just the first step towards the development of biofilms, but biofilm formation has an energetic cost and microbes cannot afford to be removed accidentally from a site they have spent energy to find out. Therefore, once they have chosen a suitable place for the living (because of nutrient, oxygen, and water availability, and for pH and redox conditions), they need to ensure their adhesion to that site.

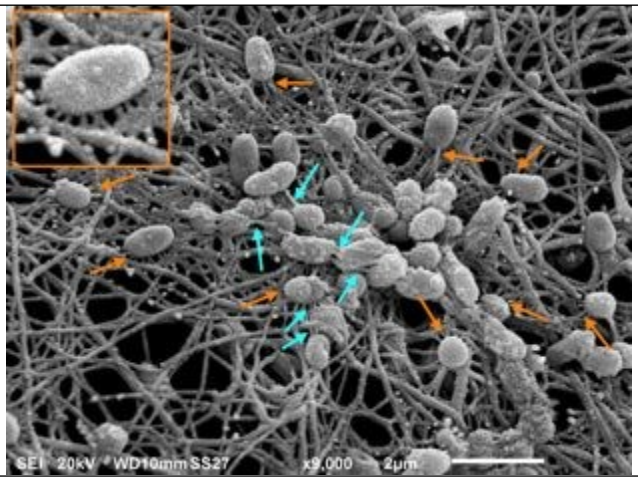

Figure 7. Type2-interaction: SEM micrographs of the nanofibrous PCL scaffold after 21 h incubation in the *B. terricola* cells suspension: orange arrows = fimbriae connecting bacteria with the nanofibres coated with the conditioning film and with EPS; light blue arrows = fimbriae connecting bacteria with other bacteria coated with and embedded in the EPS matrix. Scale bar = 2 µm.

As a consequence, after the initial phase of reversible cycles of adhesion (unspecific or specific) and detachment that bacteria use to sense and explore the substratum,[49] the microbes tend in a second phase to fix firmly and irreversibly to surfaces to maintain contact with the substratum, where nutrients accumulates,[2] before starting an extensive colonisation and the development of biofilms.[1] Once identified a suitable site for colonisation, bacteria activate many genes, some of which are switched on/off by the contact of cells with surfaces, aimed at accomplishing this irreversible attachment to surfaces (e.g. through the synthesis and exposition of proteins at bacteria surfaces, the assembling of adhesins into outward hair-like proteinaceous appendages called pili or fimbriae and the synthesis and release of exopolymeric substances - EPS), and finally facilitating the intercellular adhesion to form microcolonies.[61]

In the nanofibrous electrospun PCL scaffolds colonised by *B. terricola* cells, appendage-mediated interactions like fimbriae/pili (Type2-interactions) were displayed in SEM micrographs (Fig. 7, orange arrows) as uniformly protruding from all around the body of bacteria (peritrichous pili), as it has also been observed in several species of the genus *Burkholderia*.[90] Fimbriae are thin, rigid, rod-like, fibrillar structures assembled from one or more protein subunits called pilins. Fimbriae protrude from bacterial cells and mostly present the adhesive capacity localised at the tip.[91] They have diameters ranging from 3 to 10 nm and variable length (1-4 µm on average) until 10 µm, which have been related to adhesion but also to motility, colonisation, invasion and virulence during infection of host cells and biofilm development.[92] These appendages are usually included within both the specific and unspecific mechanisms of adhesions.[61,64] The fimbriae displayed in SEM and TEM micrographs of this study seemed to be about 3 nm diameter and until 600 nm length (Fig. 7, orange and light blue arrows and Figs. 8 and 9, green and purple arrows).

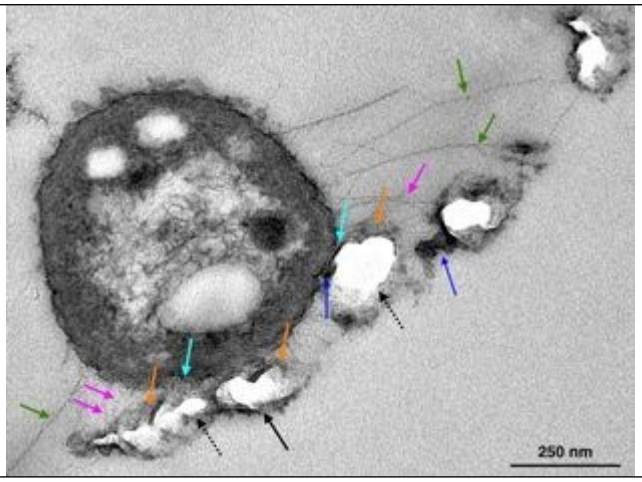

Fig. 8. Type1- and Type2-interactions: TEM micrographs of the nanofibrous PCL scaffold after 21 h incubation in the *B. terricola* cells suspension. TEM micrograph displays a single bacteria interacting with several nanofibre of various diameters; light blue arrows = gel like amorphous materials involved in the reversible adhesion of the cell onto the nanofibre (Type1-interactions); green arrows = fimbriae protruding from the cell and adhering to the nanofibres (here appearing as white spots because due to the transversal cross-cutting during the preparation of the sample) (Type2-interactions); blue arrows = OMVs adhering to a nanofibre and in the interspace between the bacteria and a nanofibre. Scale bar = 250 nm.

The approximately radial distribution of the fimbriae originating from the bacteria towards several nanofibres all around (Fig. 7) suggested that they plaid a role in anchoring the cells to the nanofibres of the electrospun framework (orange arrows) instead of in cell motility characterised by the polarity in the appendage distribution (Fig. 9, orange arrows). The anchorage role of these appendages was further supported by TEM micrographs (Figs. 8, 9, green arrows), where a high number of fimbriae were shown

protruding from bacteria cells and tying them to many nanofibres (here visible as white holes that represent orthogonal cross-sections of nanofibres, generated during the preparation of the sample). Interestingly, multiple appendages appeared as binding the same nanofibre, to make their anchorage to the substrate very stable (Fig. 8 pink arrows). This observation was further confirmed in the TEM micrograph of Fig. 9, where a quantity of fimbriae (green arrows) in radial distribution formed a sort of web joining the bacteria to a single thin nanofibre (20 nm diameter) located 100-300 nm far from the cells (here appearing as a grey thread representing the longitudinal cross-section of the nanofibre. This web of fimbriae interlaced also the OMVs released by bacteria (Fig. 9, blue arrows). Such a multiple anchoring was reasonably induced in bacteria because of the stirring conditions used during the incubation so that the only bacteria rapidly developing more tenacious anchorage and strongly adhering to nanofibres were those able to persist attached to the nanostructured fabrics for extended periods. This strong anchorage suggested that bacteria movements on the nanoframeworks after long periods of incubation might be reduced.

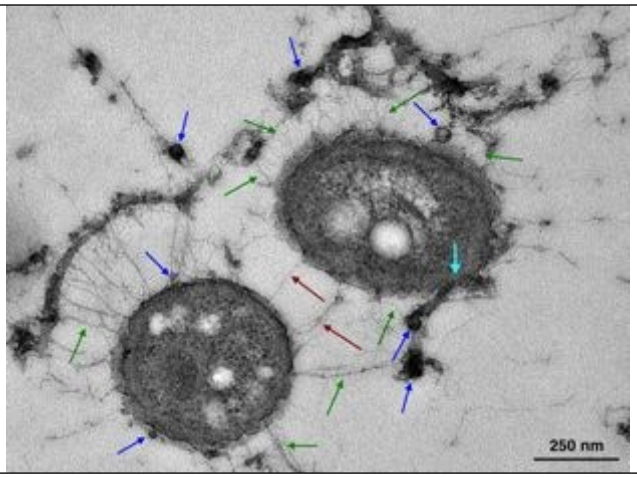

Fig. 9. Type2-interaction: TEM micrographs of the nanofibrous PCL scaffold after 21 h incubation in the *B. terricola* cells suspension: green arrows = single and network of fimbriae connecting bacteria with a single nanofibre coated with the conditioning film; purple arrows = fimbriae connecting bacteria each others; blue arrows = OMVs adhering to nanofibres, in the interspace between bacteria and nanofibres, and on the cell surface of bacteria soon after their generation; light blue arrow = contact point between a bacteria and a nanofibre showing no material present in-between the two entities. Scale bar = 250 nm.

However, the Type IV pili present in the *Burkholderia* genus have been commonly associated with the extension, tethering and retraction mechanisms typical of the twitching motility of these bacteria.[92–94] These actions, if applied to the configuration of fimbriae here observed, suggested the presence of coordinated movements like for spider legs to permit the translocation of bacteria towards specific directions, but this hypothesis should be proven. These TEM micrographs captured after 21 h incubation further confirmed that when the direct interaction of bacteria cells to nanofibres occurred (Figs. 8 and 9, light blue arrows), this contact was also mediated by the gel-like amorphous material of the bacterial capsule-like matter and the CF deposited on the nanofibres (Fig. 8 orange arrows), and that the spacing between the two entities was ≤50 nm suggesting the presence of specific mechanisms involved. Incidentally, the bacteria cell-to-nanofibre interaction displayed in Fig. 8 further confirmed that when the adhesion occurred through a longitudinal alignment the nanofibre was central to the bacteria cell (Fig. 8 solid black arrow), as described in previous images (Figs. 4 and 5), although other adjacent fibres were also binding the cell in this case. The prevalent interaction between bacteria and ≤100 nm wide nanofibres was also further confirmed (Fig. 8 black arrows). Therefore, both SEM (Fig. 7) and mostly TEM micrographs (Figs. 8 and 9) suggested that while Type2-interactions by fimbriae were used by *B.*

View Article Online
DOI: 10.1039/C8EN01237G

terricola cells to anchor themselves to the nanofibrous substrate at quite at a considerable distance (≤300 nm), Type1-interactions seemed to be involved in the bonding when a direct contact occurred (Figs. 8 and 9, light blue arrows; Fig. 4). This evidence seemed to prove that the accomplishment of Type2-interactions was not aimed necessarily at replacing the Type1 binding, but they were just addressed to strengthen the attachment of bacteria to substrates.

3.3.2 - TYPE3 Interaction - EPS release

Comparing the SEM micrographs of the electrospun PCL nanofabrics colonised by *B. terricola* cells captured after 4 h and 21 h incubation (Figs. 2, 7 and 10), the main difference between the two types of bacteria clusters displayed therein was that in the former picture the clusters were made up of transient aggregation of cells, with no stable anchorage to nanofibres (except rare cases - Fig. 3) and only apparent chemically-driven cell communications (absence of fimbrial connections between cells) (Fig. 2).

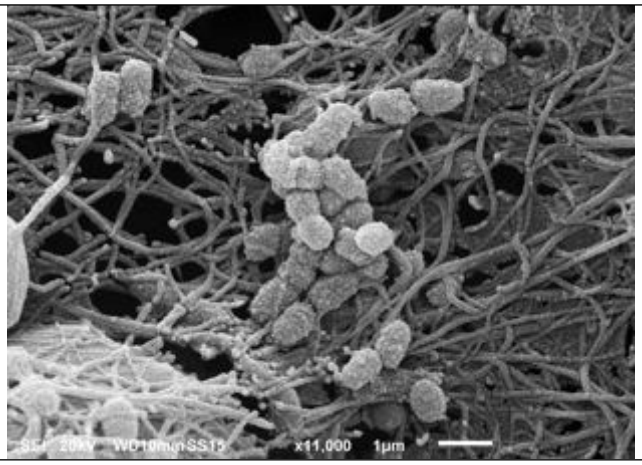

Fig. 10. SEM micrograph showing the formation of microcolonies of *B. terricola* onto the electrospun PCL nanofibrous scaffold after 21 h incubation consequent to bacteria cell communication, approaching, connection, EPS release and reproduction processes. Scale bar = 1 μm.

On the contrary, in the SEM micrographs reported in Fig. 7 and mostly in Fig. 10, a more stable anchorage of *B. terricola* cells to nanofibres was observed and included fimbriae and the presence of a gel-like/amorphous EPS matrix embedding the cells. The production of EPS is known to be the primary factor that contributes to the transition from reversible to irreversible adhesion of bacteria to surfaces and then to the development of biofilms.[1] The global amount of EPS in the biofilms has been estimated to be in the range 50-90% of the total organic carbon.[49] EPS composition often differs in distinct bacterial species,[67] and it mainly consists of polysaccharides, proteins (both enzymatic and non-enzymatic), extracellular DNA (eDNA), phospholipids, and humic substances that all together form a matrix embedding and firmly joining bacteria cells to the CF, to each other and substrates.[67] It is clear then that the synthesis and release of EPS has an energetic cost for the bacteria population and must both follow a stable adhesion of bacteria to surfaces and also be under strict regulation. The anchorage of bacteria cells to surfaces mediated by appendages like fimbriae or pili is then the necessary precondition for EPS production and the following irreversible adhesion to occur.[95] Both these conditions seemed to be fulfilled in this study (Figs. 7 and 10).

Additionally, both SEM but more specifically TEM micrographs reported in Fig. 7 (light blue arrows) and Fig. 9 (purple arrows) showed that apparently similar fimbrial appendages seemed also connecting bacteria cells not only to nanofibres but also to other bacteria. Type IV pili, which are also expressed in *Burkholderia* spp.,[93] have been reported to represent multifunctional bacteria appendages with 5-7 nm

diameter and several µm lengths that can bind to a variety of surfaces including abiotic ones, but also other bacteria and eukaryotic cells.[61] Moreover, cable pili have been reported in *B. cepacia* and *B. cenocepacia* to be involved in cell-to-cell interactions, additionally to host cell infection.[90] Therefore, the fimbriae protruding from bacteria here observed were apparently involved in both the attachment of *B. terricola* cells to nanofibres and the communications between bacteria in the early stages of incubation preceding the biofilm set up (Figs. 2 and 3). Further molecular studies are required to clarify if differences are present in the structure and composition of these two functionally distinct appendages. Fig. 7 and mostly Fig. 10 also displayed that aggregation of bacteria cells started to be present on the electrospun PCL scaffold. As a consequence of a more stable attachment to surfaces, in fact, bacteria usually started forming microcolonies by clonal growth, thus constituting the basic structural units for biofilm formation.[1,51]

Fig. 7 and mostly Fig. 10 showed that the released EPS formed a matrix encompassing bacteria and nanofibres and merging them in aggregates (microcolonies). The series of events such as the adhesion of *B. terricola* cells to the fabricated PCL nanofibrous scaffolds, their alignment onto the nanofibres, their elongation and replication (Fig. 2 light blue and orange arrows, respectively), their metabolically active state throughout the tested period (Fig. 1b) and finally the aggregation of bacteria to form microcolonies proved that no apparent inhibition was present in the bacteria population until this stage. On the contrary, all studies on bacteria interactions with nanofibres and most of those on bacteria interacting with other linear nanostructures reported inhibitory effects on microbial populations[77]. Hence, the electrospun nanofibrous PCL fabrics that were fabricated in the present study demonstrated to be capable of stably hosting active microorganisms to be employed for possible further applications, without altering the processes usually driving to biofilm development, at least in the initial stages. Experiments are in progress to test the capacity of these nanofibrous structures to support the formation of a proper mature biofilm.

4 - CONCLUSIONS

This study aimed at testing the possibility for bacteria to interact with and adhere to fibres with nanoscale dimensions, differently from what published to date in the scientific literature, to the best of our knowledge. The novelty of this study is that fibres with nanosized diameters so to be classified appropriately as nanomaterials (i.e. ≤100 nm in at least one of the three spatial dimensions) were used to test the possible effects on the adhesion of bacteria with a much larger diameter. In all published studies to date, fibres with hundreds of nanometres to some micrometres diameters have been used in experiments with bacteria, to the best of our knowledge. Specifically, PCL fibrous scaffolds composed of nanofibres with average ≈64 nm diameter were created by electrospinning and incubated with *B. terricola* cells. Differently from the published studies, the fabricated nanofibrous fabrics were coated with a ≈15 nm thick conditioning film secreted by bacteria during the incubation to facilitate their adhesion to nanofibres. This coating consequently changed the surface morphology (from smooth to rough) and the physicochemical properties of the pristine material so that the resulting nanofibres were characterised by an average diameter of ≈96 nm and a range of 22-300 nm. Because of the new features of the nanofibrous materials, maybe, bacteria cells preferentially adhered to 20-180 nm wide nanofibres and mostly to those with 99 nm diameter so that the bacteria-to-nanofibre (BFR) ratio resulted in being as large as BFR = 5.2, with a maximum of BFR = 25. Differently, the BFR values calculated in published studies ranged from 0.03 to 1.7, with a single case where it was ≈7. The values we observed in the present study were also much higher than those calculated in published studies where linear

nanotopography motifs were analysed in details in interactions with bacteria (BFRs = 0.6-2.0). Additionally, we also observed for the first time to the best of our knowledge that specific interactions occurred at this early stage of association between bacteria and nanofibres. These interactions also involved other factors like the OMVs, which appeared as binding directly to the pristine materials, i.e. without any interposition and mediation of the CF, thus suggesting they were released before CF deposition. OMVs also seemed directly participating somehow the interactions between electrospun PCL nanofibres and *B. terricola* cells. These findings, then, suggested a possible role of OMVs in both the formation of the CF (maybe upon the release outwards of the OMV internal material) and the adhesion of bacteria on nanofibres. Differently from published papers, we observed that at later stages of colonisation (21 h), *B. terricola* cells also displayed more stable interactions with the PCL nanofibrous framework mediated by fimbriae, which appeared as providing stronger anchorage to bacteria on the nanofibres and connections between cells, additionally to EPS formation. This more stable adhesion combined with orientation and movement of cells (twitching or gliding motility) permitted the formation of microcolonies as basic units for further biofilm development. Therefore, the usual events of surface colonisation by bacteria preceding the formation of biofilms were confirmed to occur when *B. terricola* cells colonised the electrospun PCL fibrous matrix consisting of nanofibres with average pristine diameter <65 nm, without any evident inhibiting effect on the adhesion, proliferation and vitality of the bacterial cells.

All of these findings can have remarkable potential on the creation of advanced nanofibrous materials for various applications. The presence of ≤100 nm nanofibres will result in scaffolds with an enormous surface area suitable for hosting large amounts of microorganisms for applications of interest. The creation of 3D self-standing scaffolds, like in the present study, will further magnify this feature and also the easy handling of the final nanofabrics by the final users (e.g. farmers). Additionally, various combinations of valuable bacteria species and polymer fibres with different chemistry displaying distinct suitable BFR values could be selected to facilitate or limit the adhesion of specific microbial strains to surfaces. These results could also assist in the future development of biofilms and together with the employment of biodegradable and biocompatible materials could contribute to creating more efficient, eco-friendly and safe materials for target low-impact applications. Examples of such applications could include the creation of target-specific biostimulants and biopesticides to be used in agriculture (replacing broad-spectrum synthetic chemical pesticides inducing resistance in target and non-target organisms), more efficient microbial fuel cells, selective materials for wastewater treatment and other environmental applications, bioreactors, specific biochemical catalysis, materials for biomedical applications (e.g. probiotics for restoration of gut microbiota), filtration, and so further. Oppositely, materials could be created aimed at reducing or preventing the adhesion of bacteria by tuning the size of fibres (in addition to materials) and then acting as antimicrobials for the biocontrol of pathogen-induced diseases in both agriculture and medicine. Moreover, the fibre size-based promotion or prevention of bacterial adhesion and surface colonisation could be further combined with specific designs of the surface chemistry of fibres. The creation of specific OMVs loaded with compounds of interest could also be used in combination with the nanofibres of tailored size to create more effective fibre-based nanotopography materials aimed at inducing or hindering bacterial adhesion and biofilm formation on materials for applications of interest.

Further research studies might include analyses of interaction mechanisms based on the use of AFM and related modifications single cell force spectroscopy (SCFM)[65,96] as well as molecular analyses identifying the possible involvement of specific receptors on the bacterial cells, or the quorum sensing mechanisms of bacterial communication, and chemical analyses of the CF and EPS materials secreted on purpose by *B. terricola* in similar incubations. Other researches could be focused on the mechanical properties of

the nanofibres, for example, the flexural rigidity[97], and the charge density of the fibres[98] and their effects on the interactions with the CF and the adhesion of *B. terricola* cells with PCL nanofibres. Macroscopic aspects such as the nanofibrous scaffold porosity and typical pore size could be further investigated to assess possible effects on such interactions.

View Article Online
DOI: 10.1039/C8EN01237G

CONFLICTS OF INTEREST

There are no conflicts to declare.

ACKNOWLEDGEMENTS

The authors gratefully acknowledge Dr. A.R. Taddei for sample preparations for Scanning Electron Microscopy (SEM) and Transmission Electron Microscopy (TEM) and investigations at the Electron Microscopy Section of the High Equipment Centre, at Tuscia University (Viterbo, Italy). The authors further thank the COST Action MP1206 “Electrospun nano-fibres for bio inspired composite materials and innovative industrial applications” that promoted the present activity and the collaboration between scientists.

5 - REFERENCES

1 W. M. Dunne, Bacterial adhesion: Seen any good biofilms lately?, *Clin. Microbiol. Rev.*, 2002, **15**, 155–166.

2 J. Palmer, S. Flint and J. Brooks, Bacterial cell attachment, the beginning of a biofilm, *J. Ind. Microbiol. Biotechnol.*, 2007, **34**, 577–588.

3 P. Gupta and B. Diwan, Bacterial Exopolysaccharide mediated heavy metal removal: A Review on biosynthesis, mechanism and remediation strategies, *Biotechnol. Reports*, 2017, **13**, 58–71.

4 K. Myszka and K. Czaczyk, in *Antimicrobial Agents*, ed. V. Bobbarala, InTech, 2012, pp. 213–238.

5 T. Danhorn and C. Fuqua, Biofilm formation by plant-associated bacteria, *Annu. Rev. Microbiol.*, 2007, **61**, 401–422.

6 J. Lynch, M. Maslin, H. Balzter and M. Sweeting, Choose satellites to monitor deforestation, *Nature*, 2013, **496**, 293–4.

7 I. Ahmad and F. M. Husain, *Biofilms in plant and soil health*, Wiley Blackwell, Chichester, UK, 2017.

8 T. G. Villa and P. Veiga-Crespo, *Antimicrobial compounds: current strategies and new alternatives*, Springer-Verlag, Berlin Heidelberg, 2014.

9 Y. Yuan, M. P. Hays, P. R. Hardwidge and J. Kim, Surface characteristics influencing bacterial adhesion to polymeric substrates, *RSC Adv.*, 2017, **7**, 14254–14261.

10 M. Katsikogianni and Y. F. Missirlis, Concise review of mechanisms of bacterial adhesion to biomaterials and of techniques used in estimating bacteria-material interactions, *Eur. Cells Mater.*, 2004, **8**, 37–57.

11 K. A. Whitehead, D. Rogers, J. Colligon, C. Wright and J. Verran, Use of the atomic force microscope to determine the effect of substratum surface topography on the ease of bacterial removal, *Colloids Surfaces B Biointerfaces*, 2006, **51**, 44–53.

12 M. Kargar, J. Wang, A. S. Nain and B. Behkam, Controlling bacterial adhesion to surfaces using topographical cues: a study of the interaction of *Pseudomonas aeruginosa* with nanofiber-textured surfaces, *Soft Matter*, 2012, **8**, 10254.

13 K. Bazaka, M. V. Jacob, R. J. Crawford and E. P. Ivanova, Plasma-assisted surface modification of organic biopolymers to prevent bacterial attachment, *Acta Biomater.*, 2011, **7**, 2015–2028.

14 J. Zhang, J. Huang, C. Say, R. L. Dorit and K. T. Queeney, Deconvoluting the effects of surface chemistry and nanoscale topography: *Pseudomonas aeruginosa* biofilm nucleation on Si-based substrates, *J. Colloid Interface Sci.*, 2018, **519**, 203–213.

15 J. K. Wise, A. L. Yarin, C. M. Megaridis and M. Cho, Chondrogenic Differentiation of Human Mesenchymal Stem Cells on Oriented Nanofibrous Scaffolds: Engineering the Superficial Zone of Articular Cartilage, *Tissue Eng. Part A*, 2009, **15**, 913–821.

16 J. K. Wise, E. Zussman, A. L. Yarin, C. M. Megaridis and M. Cho, in *Nanotechnology and Regenerative Engineering - The Scaffold*, eds. C. T. Laurencin and L. S. Nair, CRC Press, Boca Raton, 2nd edn., 2014, pp. 285–303.

17 G. R. Mitchell, *Electrospinning*, Royal Society of Chemistry, Cambridge, 2015.

18 D. H. Reneker, A. L. Yarin, E. Zussman and H. Xu, Electrospinning of nanofibers from polymer solutions and melts, *Adv. Appl. Mech.*, 2007, **41**, 43–195.

19 S. Haider, Y. Al-Zeghayer, F. A. Ahmed Ali, A. Haider, A. Mahmood, W. A. Al-Masry, M. Imran and M. O. Aijaz, Highly aligned narrow diameter chitosan electrospun nanofibers, *J. Polym. Res.*, 2013, **20**, 105.

20 H. Niu and T. Lin, Fiber generators in needleless electrospinning, *J. Nanomater.*, 2012, **2012**, Article ID 725950.

21 A. Macagnano, E. Zampetti and E. Kny, *Electrospinning for High Performance Sensors*, Springer International Publishing Switzerland, 2015.

22 S. Cavaliere, *Electrospinning for Advanced Energy and Environmental Applications*, CRC Press, Boca Raton, 2015.

23 T. Uyar and E. Kny, *Electrospun materials for tissue engineering and biomedical applications : research, design and commercialization*, Woodhead Publishing Ltd, 2017.

24 S. Torres-Giner, in *Multifunctional and Nanoreinforced Polymers for Food Packaging*, ed. J. M. Lagaron, Elsevier, Cambridge, 2011, pp. 108–125.

25 M. Mirjalili and S. Zohoori, Review for application of electrospinning and electrospun nanofibers technology in textile industry, *J. Nanostructure Chem.*, 2016, **6**, 207–213.

26 Kenry and C. T. Lim, Nanofiber technology: current status and emerging developments, *Prog. Polym. Sci.*, 2017, **70**, 1–17.

27 S. Megelski, J. S. Stephens, D. Bruce Chase and J. F. Rabolt, Micro- and nanostructured surface morphology on electrospun polymer fibers, *Macromolecules*, 2002, **35**, 8456–8466.

28 S. Chen, H. Hou, F. Harnisch, S. A. Patil, A. A. Carmona-Martinez, S. Agarwal, Y. Zhang, S. Sinha-Ray, A. L. Yarin, A. Greiner and U. Schröder, Electrospun and solution blown three-dimensional carbon fiber nonwovens for application as electrodes in microbial fuel cells, *Energy Environ. Sci.*, 2011, **4**, 1417–1421.

29 O. F. Sarioglu, A. Celebioglu, T. Tekinay and T. Uyar, Evaluation of contact time and fiber morphology on bacterial immobilization for development of novel surfactant degrading nanofibrous webs, *RSC Adv.*, 2015, **5**, 102750–102758.

30 J. D. Schiffman and M. Elimelech, Antibacterial activity of electrospun polymer mats with incorporated narrow diameter single-walled carbon nanotubes, *ACS Appl. Mater. Interfaces*, 2011, **3**, 462–468.

31 K. A. Rieger, N. P. Birch and J. D. Schiffman, Designing electrospun nanofiber mats to promote wound healing – a review, *J. Mater. Chem. B*, 2013, **1**, 4531.

32 M. Abrigo, P. Kingshott and S. L. McArthur, Electrospun polystyrene fiber diameter influencing bacterial attachment, proliferation, and growth, *ACS Appl. Mater. Interfaces*, 2015, **7**, 7644–7652.

33 K. A. Rieger, R. Thyagarajan, M. E. Hoen, H. F. Yeung, D. M. Ford and J. D. Schiffman, Transport of microorganisms into cellulose nanofiber mats, *RSC Adv.*, 2016, **6**, 24438–24445.

34 C. Rumbo, J. A. Tamayo-Ramos, M. F. Caso, A. Rinaldi, L. Romero-Santacreu, R. Quesada and S. Cuesta-López, Colonization of electrospun polycaprolactone fibers by relevant pathogenic bacterial strains, *ACS Appl. Mater. Interfaces*, 2018, **10**, 11467–11473.

35 J. A. Tamayo-Ramos, C. Rumbo, F. Caso, A. Rinaldi, S. Garroni, A. Notargiacomo, L. Romero-Santacreu and S. Cuesta-López, Analysis of polycaprolactone microfibers as biofilm carriers for biotechnologically-relevant bacteria, *ACS Appl. Mater. Interfaces*, 2018, **10**, 32773–32781.

36 P. C. Papaphilippou, I. Vyrides, F. Mpekris, T. Stylianopoulos, C. A. Papatryfonos, C. R. Theocharis and T. Krasia-Christoforou, Evaluation of novel, cationic electrospun microfibrous membranes as adsorbents in bacteria removal, *RSC Adv.*, 2015, **4**, 1417–1421.

37 L. Jiang, L. Wang, N. Wang, S. Gong, L. Wang, Q. Li, C. Shen and L. S. Turng, Fabrication of polycaprolactone electrospun fibers with different hierarchical structures mimicking collagen fibrils for tissue engineering scaffolds, *Appl. Surf. Sci.*, 2018, **427**, 311–325.

38 D. Mondal, M. Griffith and S. S. Venkatraman, Polycaprolactone-based biomaterials for tissue engineering and drug delivery: Current scenario and challenges, *Int. J. Polym. Mater. Polym. Biomater.*, 2016, **65**, 255–265.

39 P. Grossen, D. Witzigmann, S. Sieber and J. Huwyler, PEG-PCL-based nanomedicines: A biodegradable drug delivery system and its application, *J. Control. Release*, 2017, **260**, 46–60.

40 F. De Cesare, E. Di Mattia and A. Macagnano, Fishing bacteria with a nanonet, *Mater. Today*, 2017, **20**, 284–285.

41 S. Chakraborty, S. Mukherji and S. Mukherji, Surface hydrophobicity of petroleum hydrocarbon degrading Burkholderia strains and their interactions with NAPLs and surfaces, *Colloids Surfaces B Biointerfaces*, 2010, **78**, 101–108.

42 S. Mohanty and S. Mukherji, Alteration in cell surface properties of Burkholderia spp. during surfactant-aided biodegradation of petroleum hydrocarbons, *Appl. Microbiol. Biotechnol.*, 2012, **94**, 193–204.

43 M. Muganu, M. Paolocci, C. Bignami and E. Di Mattia, Enhancement of adventitious root differentiation and growth of in vitro grapevine shoots inoculated with plant growth promoting rhizobacteria, *Vitis - J. Grapevine Res.*, 2015, **54**, 73–77.

44 R. A. Moore, A. Tuanyok and D. E. Woods, Survival of *Burkholderia pseudomallei* in water, *BMC Res. Notes*, 2008, **1**, 11.

45 S. Rodrigues, C. Paillard, G. Le Pennec, A. Dufour and A. Bazire, Vibrio tapetis, the causative agent of Brown Ring Disease, forms biofilms with spherical components, *Front. Microbiol.*, 2015, **6**, 1384.

46 T. I. Ladd and J. W. Costerton, 9 Methods for Studying Biofilm Bacteria, *Methods Microbiol.*, 1990, **22**, 285–307.

47 M. V. Berridge, P. M. Herst and A. S. Tan, Tetrazolium dyes as tools in cell biology: New insights into their cellular reduction, *Biotechnol. Annu. Rev.*, 2005, **11**, 127–152.

48 C.-H. Chen, S.-H. Chen, K. T. Shalumon and J.-P. Chen, Prevention of peritendinous adhesions with electrospun polyethylene glycol/polycaprolactone nanofibrous membranes, *Colloids Surfaces B Biointerfaces*, 2015, **133**, 221–230.

49 J. W. Costerton, Introduction to biofilm, *Int. J. Antimicrob. Agents*, 1999, **11**, 217–221.

50 Y. Yang, A. J. Wikieł, L. T. Dall'Agnol, P. Eloy, M. J. Genet, J. J. G. Moura, W. Sand, C. C. Dupont-Gillain and P. G. Rouxhet, Proteins dominate in the surface layers formed on materials exposed to extracellular polymeric substances from bacterial cultures, *Biofouling*, 2016, **32**, 95–108.

51 H. C. Flemming, in *Ecological Biochemistry: Environmental and Interspecies Interactions*, eds. G.-J. Krauss and D. H. Nies, Wiley-VCH Verlag GmbH & Co. KGaA, 2015, pp. 277–291.

52 M. Ribeiro, F. J. Monteiro and M. P. Ferraz, Infection of orthopedic implants with emphasis on bacterial adhesion process and techniques used in studying bacterial-material interactions, *Biomatter*, 2012, **2**, 176–194.

53 I. B. Beech, R. Gubner, V. Zinkevich, L. Hanjangsit and R. Avci, Characterisation of conditioning

layers formed by exopolymeric substances of *Pseudomonas* NCIMB 2021 on surfaces of AISI 316 stainless steel, *Biofouling*, 2000, **16**, 93–104.

54 G. Hwang, S. Kang, M. G. El-Din and Y. Liu, Impact of conditioning films on the initial adhesion of Burkholderia cepacia, *Colloids Surfaces B Biointerfaces*, 2012, **91**, 181–188.

55 G. Hwang, S. Kang, M. G. El-Din and Y. Liu, Impact of an extracellular polymeric substance (EPS) precoating on the initial adhesion of *Burkholderia cepacia* and *Pseudomonas aeruginosa*, *Biofouling*, 2012, **28**, 525–538.

56 M. Lorenzetti, I. Dogša, T. Stošicki, D. Stopar, M. Kalin, S. Kobe and S. Novak, The influence of surface modification on bacterial adhesion to titanium-based substrates, *ACS Appl. Mater. Interfaces*, 2015, **7**, 1644–1651.

57 M. C. Ribeiro, M. da Silva Fernandes, A. Yoshiteru Kuaye, R. Jimenez-Flores and M. Gigante, Preconditioning of the stainless steel surface affects the adhesion of *Bacillus cereus* spores, *Int. Dairy J.*, 2017, **66**, 108–114.

58 G. Francius, R. El Zein, L. Mathieu, F. Gosselin, A. Maul and J. C. Block, Nano-exploration of organic conditioning film formed on polymeric surfaces exposed to drinking water, *Water Res.*, 2017, **109**, 155–163.

59 T. R. Garrett, M. Bhakoo and Z. Zhang, Bacterial adhesion and biofilms on surfaces, *Prog. Nat. Sci.*, 2008, **18**, 1049–1056.

60 K. D. Park, Y. S. Kim, D. K. Han, Y. H. Kim, E. H. B. Lee, H. Suh and K. S. Choi, Bacterial adhesion on PEG modified polyurethane surfaces, *Biomaterials*, 1998, **19**, 851–859.

61 C. Berne, A. Ducret, Y. V. Brun and G. G. Hardy, Adhesins involved in attachment to abiotic surfaces by Gram-negative bacteria, *Microbiol. Spectr.*, 2015, **3**, MB-0018-2015.

62 S. L. Reckseidler-Zenteno, in *The Complex World of Polysaccharides*, InTech Open Access Publisher, 2012, pp. 127–152.

63 R. Dennehy, M. Romano, A. Ruggiero, Y. F. Mohamed, S. L. Dignam, C. Mujica Troncoso, M. Callaghan, M. A. Valvano, R. Berisio and S. McClean, The *Burkholderia cenocepacia* peptidoglycan-associated lipoprotein is involved in epithelial cell attachment and elicitation of inflammation, *Cell. Microbiol.*, 2017, **19**, e12691.

64 I. Armentano, C. R. Arciola, E. Fortunati, D. Ferrari, S. Mattioli, C. F. Amoroso, J. Rizzo, J. M. Kenny, M. Imbriani and L. Visai, The interaction of bacteria with engineered nanostructured polymeric materials: A review, *Sci. World J.*, 2014, **2014**, 410423.

65 Y. F. Dufrêne, Sticky microbes: Forces in microbial cell adhesion, *Trends Microbiol.*, 2015, **23**, 376–382.

66 Z. Jaglic, M. Desvaux, A. Weiss, L. L. Nesse, R. L. Meyer, K. Demnerova, H. Schmidt, E. Giaouris, A. Sipailiene, P. Teixeira, M. Kačániová, C. U. Riedel and S. Knøchel, Surface adhesins and exopolymers of selected foodborne pathogens, *Microbiology*, 2014, **160**, 2561–2582.

67 H. C. Flemming and J. Wingender, The biofilm matrix, *Nat. Rev. Microbiol.*, 2010, **8**, 623–633.

68 C. Florez, J. E. Raab, A. C. Cooke and J. W. Schertzer, Membrane distribution of the *Pseudomonas* quinolone signal modulates outer membrane vesicle production in Pseudomonas aeruginosa, *MBio*, 2017, **8**, e01034-17.

69 K. E. Bonnington and M. J. Kuehn, Protein selection and export via outer membrane vesicles, *Biochim. Biophys. Acta - Mol. Cell Res.*, 2014, **1843**, 1612–1619.

70 M. Toyofuku, B. Roschitzki, K. Riedel and L. Eberl, Identification of proteins associated with the *Pseudomonas aeruginosa* biofilm extracellular matrix, *J. Proteome Res.*, 2012, **11**, 4906–4915.

71 H. Yonezawa, T. Osaki, T. Woo, S. Kurata, C. Zaman, F. Hojo, T. Hanawa, S. Kato and S. Kamiya, Analysis of outer membrane vesicle protein involved in biofilm formation of *Helicobacter pylori*, *Anaerobe*, 2011, **17**, 388–390.

72 A. T. Jan, Outer Membrane Vesicles (OMVs) of gram-negative bacteria: A perspective update, *Front. Microbiol.*, 2017, **8**, 1053.

73 S. P. Diggle, S. Matthijs, V. J. Wright, M. P. Fletcher, S. R. Chhabra, I. L. Lamont, X. Kong, R. C. Hider, P. Cornelis, M. Cámara and P. Williams, The *Pseudomonas aeruginosa* 4-quinolone signal molecules HHQ and PQS play multifunctional roles in quorum sensing and iron entrapment, *Chem. Biol.*, 2007, **14**, 87–96.

74 S. P. Diggle, P. Lumjiaktase, F. Dipilato, K. Winzer, M. Kunakorn, D. A. Barrett, S. R. Chhabra, M. Camara and P. Williams, Functional genetic analysis reveals a 2-Alkyl-4-quinolone signaling system in the human pathogen *Burkholderia pseudomallei* and related bacteria, *Chem. Biol.*, 2006, **13**, 701–710.

75 H. Yonezawa, T. Osaki, S. Kurata, M. Fukuda, H. Kawakami, K. Ochiai, T. Hanawa and S. Kamiya, Outer Membrane Vesicles of *Helicobacter pylori* TK1402 are Involved in Biofilm Formation, *BMC Microbiol.*, 2009, **9**, 197.

76 R. Helbig, D. Günther, J. Friedrichs, F. Rößler, A. Lasagni and C. Werner, The impact of structure dimensions on initial bacterial adhesion, *Biomater. Sci.*, 2016, **4**, 1074–1078.

77 X. Ge, Y. Leng, X. Lu, F. Ren, K. Wang, Y. Ding and M. Yang, Bacterial responses to periodic micropillar array, *J. Biomed. Mater. Res. - Part A*, 2015, **103**, 384–396.

78 S. M. Kelleher, O. Habimana, J. Lawler, B. O'reilly, S. Daniels, E. Casey and A. Cowley, Cicada wing surface topography: An investigation into the bactericidal properties of nanostructural features, *ACS Appl. Mater. Interfaces*, 2016, **8**, 14966–14974.

79 D. P. Linklater, H. K. D. Nguyen, C. M. Bhadra, S. Juodkazis and E. P. Ivanova, Influence of nanoscale topology on bactericidal efficiency of black silicon surfaces, *Nanotechnology*, 2017, **28**, 245301.

80 X. Li, G. S. Cheung, G. S. Watson, J. A. Watson, S. Lin, L. Schwarzkopf and D. W. Green, The nanotipped hairs of gecko skin and biotemplated replicas impair and/or kill pathogenic bacteria with high efficiency, *Nanoscale*, 2016, **8**, 18860–18869.

81 H. Leonard, S. Halachmi, N. Ben-Dov, O. Nativ and E. Segal, Unraveling antimicrobial susceptibility of bacterial networks on micropillar architectures using intrinsic phase-shift spectroscopy, *ACS Nano*, 2017, **11**, 6167–6177.

82 A. I. Hochbaum and J. Aizenberg, Bacteria pattern spontaneously on periodic nanostructure arrays, *Nano Lett.*, 2010, **10**, 3717–3721.

83 H. E. Jeong, I. Kim, P. Karam, H. J. Choi and P. Yang, Bacterial recognition of silicon nanowire arrays, *Nano Lett.*, 2013, **13**, 2864–2869.

84 K. K. Sakimoto, C. Liu, J. Lim and P. Yang, Salt-induced self-assembly of bacteria on nanowire arrays, *Nano Lett.*, 2014, **14**, 5471–5476.

85 T. R. De Kievit, Quorum sensing in *Pseudomonas aeruginosa* biofilms, *Environ. Microbiol.*, 2009, **11**, 279–288.

86 S. T. Islam and T. Mignot, The mysterious nature of bacterial surface (gliding) motility: A focal adhesion-based mechanism in *Myxococcus xanthus*, *Semin. Cell Dev. Biol.*, 2015, **46**, 143–154.

87 M. Maya-Hoyos, J. Leguizamón, L. Mariño-Ramírez and C. Y. Soto, Sliding motility, biofilm formation, and glycopeptidolipid production in *Mycobacterium colombiense* strains, *Biomed Res. Int.*, 2015, **2015**, 1–11.

88 S. P. Bernier, C. Hum, X. Li, G. A. O'Toole, N. A. Magarvey and M. G. Surette, *Pseudomonas aeruginosa*-derived rhamnolipids and other detergents modulate colony morphotype and motility in the Burkholderia cepacia complex, *J. Bacteriol.*, 2017, **199**, e00171-17.

89 A. Ducret, B. Fleuchot, P. Bergam and T. Mignot, Direct live imaging of cell-cell protein transfer by transient outer membrane fusion in *Myxococcus xanthus*, *Elife*, 2013, **2013**, e00868.

90 M. Tomich and C. D. Mohr, Transcriptional and posttranscriptional control of cable pilus gene expression in *Burkholderia cenocepacia*, *J. Bacteriol.*, 2004, **186**, 1009–1020.

91 P. Aprikian, G. Interlandi, B. A. Kidd, I. Le Trong, V. Tchesnokova, O. Yakovenko, M. J. Whitfield, E. Bullitt, R. E. Stenkamp, W. E. Thomas and E. V. Sokurenko, The bacterial fimbrial tip acts as a mechanical force sensor, *PLoS Biol.*, 2011, **9**, e1000617.

92 L. L. Burrows, *Pseudomonas aeruginosa* twitching motility: type IV pili in action., *Annu. Rev. Microbiol.*, 2012, **66**, 493–520.

93 P. Yang, M. Zhang and J. D. Van Elsas, Role of flagella and type four pili in the co-migration of *Burkholderia terrae* BS001 with fungal hyphae through soil, *Sci. Rep.*, 2017, **7**, 2997.

94 J. S. Mattick, Type IV Pili and Twitching Motility, *Annu. Rev. Microbiol.*, 2002, **56**, 289–314.

95 C. L. Kirkpatrick and P. H. Viollier, Reflections on a sticky situation: How surface contact pulls the trigger for bacterial adhesion, *Mol. Microbiol.*, 2012, **83**, 7–9.

96 P. Herman-Bausier, C. Formosa-Dague, C. Feuillie, C. Valotteau and Y. F. Dufrêne, Forces guiding staphylococcal adhesion, *J. Struct. Biol.*, 2017, **197**, 65–69.

97 A. Arinstein, M. Burman, O. Gendelman and E. Zussman, Effect of supramolecular structure on polymer nanofibre elasticity, *Nat. Nanotechnol.*, 2007, **2**, 59–62.

98 M. Boas, A. Gradys, G. Vasilyev, M. Burman and E. Zussman, Electrospinning polyelectrolyte complexes: pH-responsive fibers, *Soft Matter*, 2015, **11**, 1739–1747.

FOR TABLE OF CONTENT USE ONLY

View Article Online
DOI: 10.1039/C8EN01237G